Reply to RC1: 'Review of "On the role of trend and variability of hydroxyl radical (OH) in the global methane budget"'

Comment: The manuscript first discusses the OH variability and trends in details in relation with precursor emissions and chemistry as used in the chemistry-climate models. Then the modelled OH fields, adjusted to the global mean OH in 2000, are used for CH4 modelling in a box model and a sophisticated 3D model. They show good agreement (?) between the two models for global total CH4 budgets. The manuscript is well written and would be alright for publication in ACP. I would like to draw attention of the authors to a few points as detailed below. Hope these are useful.

Response: We thank the reviewer for his/her helpful comments. All of them have been addressed in the revised manuscript. Please see our itemized responses below.

Comment: line 49: Do you need an update here? Is the present day understanding is unambiguous too?

Response: We change the sentence to (L47-49): "The tropospheric CH_4 mixing ratio has more than doubled between pre-industrial and the present day, mainly attributed to increasing anthropogenic CH_4 emissions (Etheridge et al., 1998; Turner et al. 2019)."
We add the reference: "Turner, A. J., Frankenberg, C., and Kort, E. A.: Interpreting contemporary trends in atmospheric methane, Proceedings of the National Academy of Sciences, 116, 2805-2813, 10.1073/pnas.1814297116, 2019."

Comment: line 56: The citations look to be very restricted in general in these two para of the introduction. May consider expansion. The TransCom-CH4 project was launched to underdstand the sources and sinks budget in comparison with the model transport, for example.

Response: We change the citation to "TransCom-CH4", thank you very much for pointing out this.

Comment: line 72: I am not aware of any proven issues with weakening MCF gradient. Could you pleas expand what exactly are you talking about; meridional, zonal or vertical gradients?

Response: We clarify in the text (L73-74):" ... and the weakening of inter-hemispheric MCF gradients after the 1990s (Krol et al., 2003, Bousquet et al., 2005; Montzka et al., 2011; Prather and Holmes, 2017)."

Comment: line 92: are CH4 budgets from 1980 or 1986

Response: We change the sentence to "... on decadal scale since the 1980s". and we

add in L97-98:" We finally estimate the impact of OH year to year variations and trends on the top-down estimation of global CH_4 emissions over 1986-2010". Since we analyzed the OH variation for 1980-2010 and analyzed the inversion results for 1986-2010.

Comment: line 114: There are 4 issues with OH from CCMI models; you seems to ignore the biases in meridional gradient in OH, and account for the other three (global totals, trends and IAV)

Response: In this work, we are focusing on the temporal variation of OH and the impact on CH_4. The impacts of OH inter-hemispheric gradient have been estimated in Zhao et al. (2020) and therefore less discussed in this study.

Reference:" Zhao, Y., Saunois, M., Bousquet, P., Lin, X., Berchet, A., Hegglin, M. I., Canadell, J. G., Jackson, R. B., Dlugokencky, E. J., Langenfelds, R. L., Ramonet, M., Worthy, D., and Zheng, B.: Influences of hydroxyl radicals (OH) on top-down estimates of the global and regional methane budgets, Atmos. Chem. Phys. Discuss., 2020, 1-45, 10.5194/acp-2019-1208, 2020."

Comment: line 120: Could this also mean that the variabilities you show are not from OH concentrations but due to t-dependent loss rates & dry airmass. Is it possible to tell the readers what would you expect if you scale OH concentrations themselves not weighted by k? including showing it in a 2nd column?

Response: For the scaling, we apply the single global scaling factor estimated for 2000 to every year of the OH field. Hence the scaling will not influence the interannual variation of OH. We have clarified this in the text (L116-117):" The inferred global mean scaling factors are calculated for the year 2000 and each OH field and then applied to the whole period (1980-2010)"

Comment: line 157: I fail to understand why continuous inversion were not done for the period 1994-2010, using the two OH cases. This does not seem to be for reducing computing time, given that 2 years are gone for spin-up and spin-down. Please explain. Also why you need two years of spin-up/down for the box model but only 1-year for the 3D model.

Response: We do the inversion separately for each time period so that the inversions can be run in parallel at the same time. The 3D model inversions are much more computationally expensive than the box model inversions. Hence we only take one-year spin-up and spin-down for the 3D model. We clarify in the text (L159-L160):" We only spin-up/spin-down the 4D variational inversions for one year to save computing time."

Comment: line 185: What do you mean? I see many other negative anomalies are apparently consistent among the models.

Response: We clarify this issue in the text by adding (L187-188):" Only the negative OH anomaly during 2006-2007 (2±1%) is simulated by all models during the four weak El Niño events."

Comment: line 195ff: I agree that the CH4 growth rates are more positive during the El Nino years (discussed in the TransCom-CH4 analysis too). We have to better understand the lower growth rates in CH4 during the La Nina periods - this is quite new concept. (some people talk about Mt Pinatubo for 1993 growth rate anomaly and others do not see a negative anomaly during the La Nina).

Response: Here we want to show that the CH_4 growth rate is smaller during the La Niña years comparing with their adjacent El Niño years. We make the expression more precise in the text (L96-98):" The positive anomalies of $[OH]_{GM-CH4}$ during La Niña events correspond to a much smaller CH_4 growth (e.g. 3.8±0.6ppbv yr^{-1} in 1993 and 2.3±0.8ppbv yr^{-1} in 1999) compared with that during the adjacent El Niño years (Fig. S1)."

Comment: line 200: do you need "processes" here?

Response: We remove the "processes".

Comment: line 204: Is there a reason for different unit (Tg/yr) here?

Response: We correct the typo by changing"Tg/yr" to "Tmol yr^{-1}"

Comment: line 212: should this be "different"? Do you mean the NMVOCs are not included in some of the model or the number of species differ from model to models?

Response: Here we mean the model outputs of OH loss due to reaction with NMVOCS, we clarify this in the text(L212-213):" Besides, there are 12% of OH production and 33% of OH loss not analyzed here due to lack of data in the CCMI model outputs (e.g. output of OH loss due to reaction with NMVOCs included in different models)"

Comment: line 214: My personal choice, but I would have loved to see the actual values presented in this plot. It is fine to adjust different multi-model values to a common 1980 level.

Response: We agree that it will be more straightforward to show the actual values. However, we here adjust the model values to a common 1980 to focus more on the temporal variations from 1980.

Comment: For here and elsewhere, this is specialised journal publication, there is no need for so much space restriction; I mean this can be 1-column figure is the trends are less prominent by the increase of y-axis range. Also for the x-axis tick labels, please consider reducing number of labels or elongate the x-axis or introduce minor ticks. Presently looks a bit clumsy.

Response: We plot the trends of different chemical processes in the same panel to better compare the relative contribution from each process and find out which process is most important for determining OH trend. We replot figure 1-4 to reduce x-axis tick labels as suggested.

Comment: line 220: This is a nice discussion, but I cannot assess the novelty of it given that ACCMIP and CCMI paper have discussed the OH variabilities and budgets in similar fashion, and there are papers by MPI Mainz group on the details of OH budgets. Could you please consider showing the net (P-L) OH trends in a separate panel. When you say OH loss, is the '-ve' sign in the y-tick labels appropriate and consistent with the number in the text?

Response: ACCMIP provides the model outputs for time slices (Naik et al., 2013), which limit the analysis of OH interannual variations. For the studies based on CCMI model simulations, both Zhao et al. (2019) and Nicely et al. (2020) analyzed the OH interannual variations but not the OH budget. The OH budget has already been analyzed in previous single model studies such as Murray et al. (2013; 2014) (as we cite in the manuscript) and Lelieveld et al. (2016) (paper from MPI Mainz group). But to our knowledge, few studies are analyzing the interannual variation of OH budget based on multi-model outputs.

We cite Leliveld et al. (2016) in the text (L201-203): "Here we assess the drivers of OH year-to-year variations and trend by calculating the OH production and loss processes listed in Table 2 following Murray et al. (2013; 2014) and Lelieveld et al. (2016)."

Reference:" Lelieveld, J., Gromov, S., Pozzer, A., and Taraborrelli, D.: Global tropospheric hydroxyl distribution, budget and reactivity, Atmos. Chem. Phys., 16, 12477-12493, 10.5194/acp-16-12477-2016, 2016."

Showing the net (P-L) will certainly help for better understanding the OH variations. However, only 2 of 5 models provide both total OH production and OH loss data, so we cannot give the temporal variations of net OH production and loss based on current model outputs.

For the "-ve" sign (I suppose the reviewer means "negative"), we now clarify this issue in the figure caption.

"Figure 2. Annual total OH tendency (Tmole yr^{-1}) from chemical reactions with respect to the year 1980 with year-to-year variations removed. The positive and negative tendencies represent OH production (left) and loss processes (right), respectively."

"Figure 3. Anomaly of the detrended annual global total OH tendency from reactions $O(^1D)+H_2O$, $NO+HO_2$, O_3+HO_2, and CO+OH. The positive and negative tendencies represent OH production and loss processes, respectively."

Comment: line 236: I was probably asking to present something similar in my earlier comment for OH anomaly in Fig. 1. May be it is good to show the Net OH (production - loss) variabilities as well in a separate panel here (in % change).

Response: As stated in response to the last comments, we cannot assess the net OH production and loss for most of the models due to a lack of corresponding output.

Comment: line 266: How good are the CO emission estimations and also the satellite data? I have heard some issues with the MOPITT data retrievals. Is this model comply with surface CO observations?

Response: The trend and variations of the tropospheric CO column simulated by CCMI models have been evaluated by comparison with MOPITT data retrievals (Strode et al., 2016). Here we are focusing on the OH loss by CO over the whole troposphere (instead of the surface). The consistency of CCMI simulated tropospheric CO column with MOPITT observations can support the model simulated decreasing tropospheric OH loss by reaction with CO during 2000-2010.

We add in the text (L220-222): "The negative trend of CO simulated by CCMI models during 2000-2010 is consistent with MOPITT observations over most of the regions (Strode et al., 2016)."

Despite the finding that atmospheric chemistry models generally capture the CO trend, they usually underestimate the atmospheric CO burden compared to surface and satellite observations. We add in the text (381-383): "For example, underestimation of CO, especially over the northern hemisphere, compared with the surface and satellite observations (Naik et al., 2013; Strode et al., 2016) and bias in atmospheric O_3 column (Zhao et al. 2019)."

We add the reference:" Strode, S. A., Worden, H. M., Damon, M., Douglass, A. R., Duncan, B. N., Emmons, L. K., Lamarque, J. F., Manyin, M., Oman, L. D., Rodriguez, J. M., Strahan, S. E., and Tilmes, S.: Interpreting space-based trends

in carbon monoxide with multiple models, Atmos. Chem. Phys., 16, 7285-7294, 10.5194/acp-16-7285-2016, 2016."

Comment: line 274: How good are these for accounting for the effect of the meteorology. I suppose the temperature effect is taken in to account by doing the k_oh+ch4 anomalyin Fig. 1, but there are likely to have some non-linear interaction between the transport (inter-hemispheric & stratosphere-troposphere exchange) and loss by OH. This effect may be of 2nd order but nevertheless important. Any assessment would be helpful to the readers. This is where a long-term 3-D model based inversion would have helped.

Response: The long-term 3D model inversions can certainly help better assess the impact of OH variations. However, the 3D model inversions are computationally expensive, which limits conducting long-term 3D model inversions using all of the 9 OH fields present in this study. That's why we use the two-box model to do long-term inversions and do 3D model inversions with a focus on four time periods.

We have demonstrated the advantage of both box model and 3D model inversions in the text (L130-134): "The two-box model inversions allow us to easily conduct multiple long-term global scale inversions (1984-2012) with each of the nine OH fields to estimate the global CH_4 emission variations caused by various OH fields. The 4D variational inversions allow us to better represent atmospheric transport, account for the variation of meteorological conditions, and address regional CH_4 emission distributions."

And we have compared the emission changes estimated by two-box model inversions and 3D model inversion in Figure 5, which show that (L302-L306) "Despite the limitations inherent to two-box model inversions, such as treatment of inter-hemispheric transport, stratospheric loss, and the impact of spatial variability (Naus et al., 2019), the two-box model inversion estimates similar temporal changes of CH_4 emissions and losses compare to the variational approach for the four periods, as well as their response to OH changes (Fig.5), on a global scale. Such comparisons reinforce the reliability of the conclusions made from the two-box model inversions regarding changes in the global total CH_4 budget.".

Line280 : It is obvious from this analysis that introducing OH IAV as modelled by the CCMI models will reduce the CH4 emission anomaly. What are the new questions/implications? 1) increase the wetland emission anomaly, 2) decrease biomass burning emission anomaly, 3) some missing process in the OH chemistry (recycling efficiency).

Response: We have discussed the implication on top-down estimated wetland

emissions in the "Conclusion and discussion" (L393-396): "The variational inversions using OH with temporal variations attribute the observed rising CH_4 growth during El Niño to the reduction of CH_4 loss instead of enhanced emissions over the tropics, which are consistent with process-based wetland models that estimated wetland CH_4 emission reductions at beginning of El Niño event (Hodson et al., 2011; Zhang et al., 2018)."

We also discuss the impact on top-down estimated biomass burning emissions (L400-L401): "Also, the negative OH anomaly can reduce the top-down estimated biomass burning CH_4 emission spike during El Niño events, similar to that presented in Bousquet et al. (2006)."

We discuss the implications of including full-chemistry estimated OH by comparing with previous results which only consider OH loss by CO (L362-365): "We estimated that the negative OH anomaly in 1998 reduces the high top-down estimated CH_4 emissions by 10±3Tg yr^{-1}, ~40% smaller than the reduction estimated by Butler et al. (2005) (16Tg yr^{-1}), which only include the OH reduction response to enhanced biomass burning CO emissions. The smaller CH_4 emission reductions (OH anomalies) estimated with CCMI OH fields shows the significance of considering multi chemical processes as included in the 3D atmospheric chemistry model in capturing OH variations and inverting for CH_4 emissions"

Reference: "Butler, T. M., Rayner, P. J., Simmonds, I., and Lawrence, M. G.: Simultaneous mass balance inverse modeling of methane and carbon monoxide, Journal of Geophysical Research: Atmospheres, 110, 10.1029/2005jd006071, 2005."

Comment: line 285: The most important question for the authors is then to convince the readers how you propose to increase CH4 emissions by more than 25 Tg/yr in just 3 years and keep maintaining at that level for the later years.

Response: The large emission increase after 2005 have been reported in previous studies (e.g. Kirschke et al. (2013), Saunois et al. (2017)). We compare the emission increase over the same period with previous study in the text (L279-281):" The CH_4 emissions averaged over 2006-2010 is 20Tg yr^{-1} higher than over 2000-2005, within the range of 17–22Tg yr^{-1} estimated by an ensemble of inversions in Kirschke et al. (2013)."

We add the reference: " Kirschke, S., Bousquet, P., Ciais, P., Saunois, M., Canadell, J. G., Dlugokencky, E. J., Bergamaschi, P., Bergmann, D., Blake, D. R., Bruhwiler, L., Cameron-Smith, P., Castaldi, S., Chevallier, F., Feng, L., Fraser, A., Heimann, M., Hodson, E. L., Houweling, S., Josse, B., Fraser, P. J., Krummel, P. B., Lamarque, J.-F., Langenfelds, R. L., Le Quéré, C., Naik, V., O'Doherty, S., Palmer, P. I., Pison, I., Plummer, D., Poulter, B., Prinn, R. G., Rigby, M., Ringeval, B., Santini, M., Schmidt, M., Shindell, D. T., Simpson, I. J., Spahni, R., Steele, L. P.,

Strode, S. A., Sudo, K., Szopa, S., van der Werf, G. R., Voulgarakis, A., van Weele, M., Weiss, R. F., Williams, J. E., and Zeng, G.: Three decades of global methane sources and sinks, Nature Geoscience, 6, 813-823, https://doi.org/10.1038/ngeo1955, 2013."

Comment: line 301: "assess"
Response: Changes as suggested

line 303ff: Consider adding header to each panels - again panel size could be increased for clarity. It is very hard to see the semi-hemispheric emissions in the bars. The right panel adds to the confusion how to read this plot; for me it is much easy to see what you want say from the left and middle panels.

Response: We change the figure as suggested.

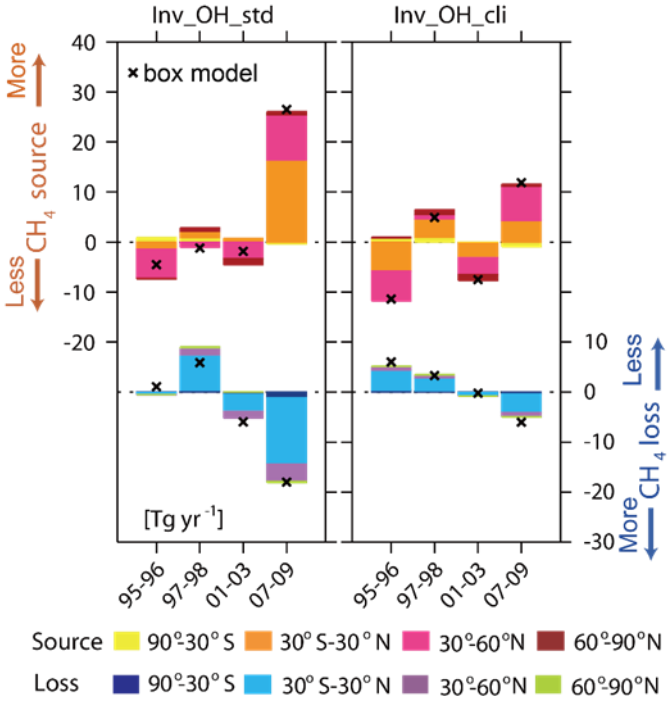

Comment: line 366: Did Prather and Holmes estimated OH variability or trends?
Response: Prather and Holmes (2017) showed uncertainties exist in the MCF-constrained OH using two-box models.

Comment: line 372: I do not know true or not true? The authors, I think, understand the trends and IAV in OH simulated by the CCMs still require much testing. Firstly the global mean OH values, which you have adjusted at the very first; the amplitude and phase of the modelled IAV may not be perfect; the longer term trends are still anyone's guess (needs at least one more line of evidence); finally there is unspoken bias in meridional gradients in the modelled OH. If a true variability and trend in OH become available there would be no issues with the top-down modellers to adopt it. There are several inversions which included the OH trends and variability like you discuss here

(e.g., McNorton et al., ACP, 2018)

Response: We discuss the uncertainties in OH simulated by atmospheric chemistry models in the text now in more detail: "However, the CCMI models still show biases that are related to OH production and loss. For example, these include an underestimation of CO especially over the northern hemisphere compared with the surface and satellite observations (Naik et al., 2013; Strode et al., 2016) and bias in atmospheric total O_3 column (Zhao et al. 2019). In addition, the changes in aerosols (Tang et al., 2003) and atmospheric circulation such as the Hadley cell expansion (Nicely et al., 2018) are not discussed in this study. Given the large discrepancy between MCF–based and CCMI model simulated OH trends, and the uncertainties in both model simulated (Naik et al., 2013; Zhao et al., 2019) and MCF-constrained (Bousquet et al., 2005; Prather and Holmes, 2017; Naus et al. et al., 2019) OH, the OH trend after the mid-2000s remains an open problem and more effort is required in both method to explore the close the gap. "

We change L372 to: "The temporal variations of OH, which are generally not well constrained in current top-down estimates of CH_4 emissions, imply potential additional uncertainties in the global CH_4 budget (Saunois et al., 2017; Zhao et al., 2020)."

Comment: line 382: Is there a better reference for El Nino in future climate? I am sure there are

Response: We change the reference to "Berner, J., Christensen, H. M., and Sardeshmukh, P. D.: Does ENSO Regularity Increase in a Warming Climate?, Journal of Climate, 33, 1247-1259, 10.1175/jcli-d-19-0545.1, 2020."

Comment: line 384: I think this is well known since the ACCMIP at the least!

Response: We change the sentence to "Our research emphasizes the importance of considering climate changes and chemical feedbacks related to OH in future CH_4 budget research."

Reply to RC2: 'Referee comments'

This study investigates the impact of CCM calculated OH fields on the long-term trend and interannual variability in global methane emissions as inferred from atmospheric inversions. It is concluded that accounting for the CCM simulated trend in OH implies a significantly larger increase in methane emissions in the past decades than previous estimates that did not consider changes in OH. In addition, correlations between OH variations and El Nino are found that reduce the variability in inferred emission, notably in the Tropics. The manuscript, that is well written, provides a useful contribution to the scientific discussion on the drivers of the global increase of methane, contrasting the view on the role of OH that follows from the more common use of MCF. The study also mentions important limitations of using MCF, suggesting that the CCM-derived OH scenario is more consistent. However, in my opinion the evidence in support of this suggestion is very limited. Besides this point, there are a few other points that need further attention as explained below. Overall, only minor revisions will be needed to accept this paper for publication.

Response: We thank the reviewer for his/her helpful comments. We have now discussed the limitations of the CCMI-derived OH in more detail in the text. All of the other comments have been addressed in the revised manuscript. Please see the itemized responses below.

Comment: The study provides an analysis of the main drivers of variability and trends in OH using output from the CCMs. It is mentioned that both chemical and climatological influences are considered. However, the budget that is provided in Table 2 only lists chemical drivers. A study by Dentener et al (ACP, 1993) (which would be worth referencing in this context) identified an important contribution of meteorology on OH variability. Apart from changes in water vapour, those influences, including temperate and changes in circulating, are not discussed here.

Response: Dentener et al. showed that water vapor is the main meteorological driver of OH trend during 1979-1993. Our analysis also shows that the increase of water vapor can contribute to a positive OH trend by enhancing OH primary production (L217-L219): "The increase in OH primary production is due to an increase in both tropospheric O_3 burden (producing $O(^1D)$) and water vapor (Dentener et al 2003; Zhao et al., 2019; Nicely et al., 2020)."

The impact of water vapor on OH variability is also discussed in the manuscript (L246-L248): "The increase in OH primary production is mainly due to an increase in tropospheric water vapor and O_3 burden during El Niño events (Fig.S3 and S12 in Nicely et al. (2020)), while the increase in OH secondary production is caused by enhanced NO_x emissions (Fig.S3) and O_3 formation (Nicely et al. (2020) related to biomass burning as well as more HO_2 formation by CO+OH."

The temperature mainly influences the reaction rates of OH with other chemical species (CO, CH4, NMVOC, etc.), which is included in our estimation of OH production and loss (Table S1). Nicely et al. (2018; 2020) have proven that temperature has a neglectable impact on OH trend.

Due to a short lifetime, the OH is controlled by local production and loss, thus less directly impacted by atmospheric transport. Nicely et al. (2018) shown that the Hadley cell expansion can have a small impact on tropospheric mean [OH] through changing tropopause height. We add this point in the text (L380-383): "In addition, the changes in aerosols (Tang et al., 2003) and atmospheric circulation such as Hadley cell expansion (Nicely et al., 2018) are not discussed in this study."

We also add the following references:
"Dentener, F., Peters, W., Krol, M., van Weele, M., Bergamaschi, P., and Lelieveld, J.: Interannual variability and trend of CH4 lifetime as a measure for OH changes in the 1979–1993 time period, Journal of Geophysical Research: Atmospheres, 108, 4442, 10.1029/2002jd002916, 2003."
" Nicely, J. M., Canty, T. P., Manyin, M., Oman, L. D., Salawitch, R. J., Steenrod, S. D., Strahan, S. E., and Strode, S. A.: Changes in Global Tropospheric OH Expected as a Result of Climate Change Over the Last Several Decades, Journal of Geophysical Research: Atmospheres, 123, 10,774-710,795, doi:10.1029/2018JD028388, 2018."

Comment: The discussion of the results rightly mentions the different outcomes obtained using MCF or CCM derived OH, and their significance for global methane. From the evidence that is presented it is not possible in my opinion to conclude which of the views is right. Nevertheless, the conclusion section mentions that 'the evidence for increasing OH given by CCMI models and other literature, the accuracy of MCF-based OH inversions after the mid-2000s remains an open problem'. So, in short, the accuracy of MCF is the "open problem" that could explain the disagreement in the opinion of the authors. However, the consistency between CCM's itself cannot be considered as evidence, since these models are not independent and could therefore all be wrong for the same reason. To give an example that might introduce important uncertainty in CCM derived variations, the role of changes in aerosols on OH is not discussed at all. Either appropriate evidence should be presented of CCM's being more accurate than MCF or a more objective position should be taken regarding this question.

Response: We try to discuss the two methods in the text now in a more balanced way:

"However, the CCMI models still show biases that related to OH production and loss. For example, underestimation of CO especially over the northern hemisphere compared with the surface and satellite observations (Naik et al., 2013; Strode et al., 2016) and bias in atmospheric total O_3 column (Zhao et al. 2019). In addition,

the changes in aerosols (Tang et al., 2003) and atmospheric circulation such as Hadley cell expansion (Nicely et al., 2018) are not discussed in this study. Given the uncertainties in both atmospheric chemistry model simulated (Naik et al., 2013; Zhao et al., 2019) and MCF-constrained OH (Bousquet et al., 2005; Prather and Holmes, 2017; Naus et al. et al., 2019), and the large discrepancy between two methods, the OH trend after the mid-2000s remains an open problem and more effort is required in both method to close the gap. ”

We add the references:
“Strode, S. A., Duncan, B. N., Yegorova, E. A., Kouatchou, J., Ziemke, J. R., and Douglass, A. R.: Implications of carbon monoxide bias for methane lifetime and atmospheric composition in chemistry climate models, Atmos. Chem. Phys., 15, 11789-11805, 10.5194/acp-15-11789-2015, 2015.”
” Tang, Y., Carmichael, G. R., Uno, I., Woo, J.-H., Kurata, G., Lefer, B., Shetter, R. E., Huang, H., Anderson, B. E., Avery, M. A., Clarke, A. D., and Blake, D. R.: Impacts of aerosols and clouds on photolysis frequencies and photochemistry during TRACE-P: 2. Three-dimensional study using a regional chemical transport model, Journal of Geophysical Research: Atmospheres, 108, 8822, 10.1029/2002jd003100, 2003.”

SPECIFIC COMMENTS
Comment: line 38, 40: the numbers that are mentioned in these sentences lack an uncertainty estimate.

Response: We change “up to 10Tg yr^{-1}” to “up to 10±3Tg yr^{-1}” and “increase by 23Tg yr^{-1}” to “increase by 23±9Tg yr^{-1}”.

Comment: line 148: How is Inv_OH_var detrended?

Response: We clarify in the text “Inv_OH_var stands for the inversion using the detrended OH”.

Comment: line 249: What is meant by ’response of OH to CO.’?

Response: We clarify by changing the “response of OH to CO” to “response of OH to enhanced CO emissions during the El Niño events”.

Comment: line 253: Banda et al 2016 is a good reference to add here for the effect of Mt. Pinatubo.

Response: Thank you very much for providing this valuable reference. We revise the sentence to:” The positive anomaly OH primary production (0.2±0.5Tmol yr^{-1}) is not significant during 1991-1992 El Niño event, maybe due to absorption of ultraviolet (UV) by volcanic SO_2 and scattering of UV by sulfate aerosols as well

as reduction of tropospheric water vapor after the eruption of Mount Pinatubo (Bândă et al., 2016; Soden et al., 2020).”

We add reference:” Bândă, N., Krol, M., van Weele, M., van Noije, T., Le Sager, P., and Röckmann, T.: Can we explain the observed methane variability after the Mount Pinatubo eruption?, Atmos. Chem. Phys., 16, 195-214, 10.5194/acp-16-195-2016, 2016.”

Comments: line 280-283: Similar conclusions on emission anomalies during El Nino were drawn by Butler et al, JGR, 2005, which would be useful references and comparing here.

Response: we add in the text (L358-L363): ” We estimated that the negative OH anomaly in 1998 reduces the high top-down estimated CH_4 emissions by 10±3Tg yr^{-1}, ~40% smaller than the reduction estimated by Butler et al. (2005) (16Tg yr^{-1}), which only include the OH reduction response to enhanced biomass burning CO emissions. The smaller CH_4 emission reduction (OH anomaly) estimated with CCMI OH fields may reflect the significance of considering multi chemical processes as included in the 3D atmospheric chemistry model in capturing OH variations and inversing CH_4 emissions.”

Comment: Figure 3: what do the lines represent in this figure represent? Figure 5: Emission anomalies are shown compared to what? Initially I assumed that the mean was subtracted. However, the bars for the different time slices don’t add up to zero.

Response: we add the legend in Figure 3 as shown below. The anomalies in Figure 5 are calculated by comparing to the mean CH_4 emissions of Inv_OH_cli over the four time period as demonstrated in the figure caption, we add the value “494Tg” in the figure caption to clarify.

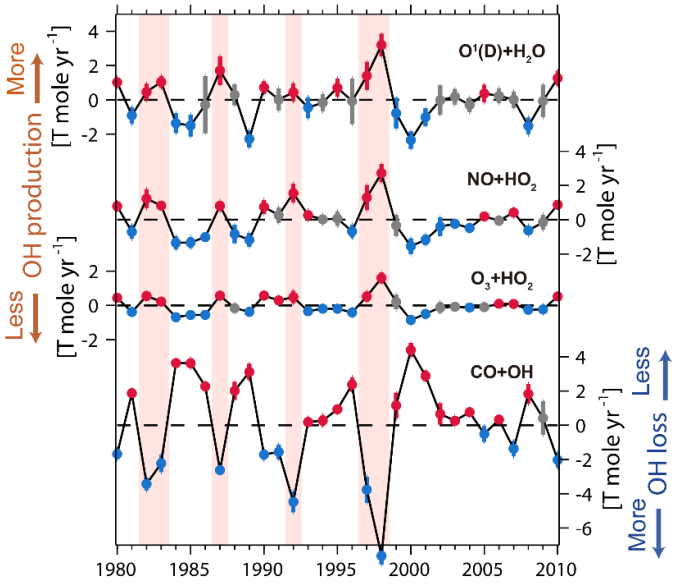

TECHNICAL CORRECTIONS
Comment: line 119: ’For each OH field’ io ’ .. fields’

Response: Changed as suggested

Comment: line 122: The parenthesis in this sentence should be fixed.

Response: We change the parenthesis to “([OH]$_{GM-CH4}$, weighting factor = reaction rate of OH with CH_4 × dry air mass, Lawrence et al., 2001) as well as of its production and loss rates.”

Comments:
line 170: ’This continuous increase in’ io ’This continuously increases in’, and ’based on MCF inversions’ io ’based in the MCF inversions’
line 205: ’NO+HO2’ io ’NO+NO2’
line 249: ’anomaly in OH primary’ io ’anomaly OH primary’
line 250: ’during the 1991-1992..’ io ’during 1991-1992..’
line 322: ’the Tropics’ io ’the tropics’
line 324: ’twice that of the inversion’ io ’twice of the inversion’
line 334: ’and their impact’ io ’and its impact’

Response: The above technical corrections are changes as suggested. Thank you very much for pointing out these.

Reply to SC1: 'A typo in the paper'

Comment: In line 204, "Of the total OH production, 46% (96.2 ±1.9Tg yr-1) ". The unit should be "Tmol yr-1"?

Response: We have changed the unit to "Tmol yr^{-1}" in the text. Thank you very much for pointing out this.

On the role of trend and variability of hydroxyl radical (OH) in the global methane budget

Yuanhong Zhao[1], Marielle Saunois[1], Philippe Bousquet[1], Xin Lin[1*], Antoine Berchet[1], Michaela I. Hegglin[2], Josep G. Canadell[3], Robert B. Jackson [4], Makoto Deushi[5], Patrick Jöckel[6], Douglas Kinnison[7], Ole Kirner[8], Sarah Strode[9, 10], Simone Tilmes[11], Edward J. Dlugokencky[12], and Bo Zheng[1]

[1] Laboratoire des Sciences du Climat et de l'Environnement, LSCE-IPSL (CEA-CNRS-UVSQ), Université Paris-Saclay, 91191 Gif-sur-Yvette, France

[2] Department of Meteorology, University of Reading, Earley Gate, Reading RG6 6BB, United Kingdom

[3] Global Carbon Project, CSIRO Oceans and Atmosphere, Canberra, Australian Capital Territory 2601, Australia

[4] Earth System Science Department, Woods Institute for the Environment, and Precourt Institute for Energy, Stanford University, Stanford, CA 94305, USA

[5] Meteorological Research Institute, 1-1 Nagamine, Tsukuba, Ibaraki, 305-0052, Japan

[6]Deutsches Zentrum für Luft- und Raumfahrt (DLR), Institut für Physik der Atmosphäre, Oberpfaffenhofen, Germany

[7]Atmospheric Chemistry Observations and Modeling Laboratory, National Center for Atmospheric Research, 3090 Center Green Drive, Boulder, CO, 80301, USA

[8] Steinbuch Centre for Computing, Karlsruhe Institute of Technology, Karlsruhe, Germany

[9] NASA Goddard Space Flight Center, Greenbelt, MD, USA

[10] Universities Space Research Association (USRA), GESTAR, Columbia, MD, USA

[11] National Center for Atmospheric Research, Boulder, CO, USA

[12] Global Monitoring Division, NOAA Earth System Research Laboratory, Boulder, CO,

[*] Now at: Climate and Space Sciences and Engineering, University of Michigan, Ann Arbor, MI 48109, USA

Correspondence to: Yuanhong Zhao (yuanhong.zhao@lsce.ipsl.fr) and Bo Zheng (bo.zheng@lsce.ipsl.fr)

Abstract

Decadal trends and interannual variations in the hydroxyl radical (OH), while poorly constrained at present, are critical for understanding the observed evolution of atmospheric methane (CH_4). Through analyzing the OH fields simulated by the model ensemble of the Chemistry-Climate Model Initiative (CCMI), we find (1) the negative OH anomalies during the El Niño years mainly corresponding to the enhanced carbon monoxide (CO) emissions from biomass burning and (2) a positive OH trend during 1980-2010 dominated by the elevated primary production and the reduced loss of OH due to decreasing CO after 2000. Both two-box model inversions and variational 4D inversions suggest that ignoring the negative anomaly of OH during the El Niño years leads to a large overestimation of the increase in global CH_4 emissions by up to $10 \pm 3 Tg\ yr^{-1}$ to match the observed CH_4 increase over these years. Not accounting for the increasing OH trends given by the CCMI models leads to an underestimation of the CH_4 emission increase by $23 \pm 9 Tg\ yr^{-1}$ from 1986 to 2010. The variational inversion estimated CH_4 emissions show that the tropical regions contribute most to the uncertainties related to OH. This study highlights the significant impact of climate and chemical feedbacks related to OH on the top-down estimates of the global CH_4 budget.

1 Introduction

Methane (CH_4) in the Earth's atmosphere is a major anthropogenic greenhouse gas that has resulted in a 0.62 W m^{-2} additional radiative forcing from 1750 to 2011 (Etminan et al., 2016). The tropospheric CH_4 mixing ratio has more than doubled between pre-industrial and the present day, mainly attributed to increasing anthropogenic CH_4 emissions (Etheridge et al., 1998; Turner et al. 2019). Although the centennial and inter-decadal trends and the drivers of CH_4 growth are fairly clear, it is still challenging to understand the trends and the associated interannual variations on a time scale of 1-30 years. For example, the mysterious stagnation in CH_4 mixing ratios during 2000-2007 (Dlugokencky, NOAA/ESRL, 2019) is still under debate, highlighting the need for closing gaps in the global CH_4 budget on decadal time scales (e.g. Turner et al., 2019).

One of the barriers to understanding atmospheric CH_4 changes is the CH_4 sink, which is mainly the chemical reaction with the hydroxyl radical (OH) (Saunois et al., 2016; 2017; 2019; Zhao et al., 2020) that determines the tropospheric CH_4 lifetime. The burden of atmospheric OH is determined by complex and coupled atmospheric chemical cycles influenced by anthropogenic and natural emissions of multiple atmospheric reactive species, and also by climate change (Murray et al., 2013; Turner et al., 2018, Nicely et al., 2018), making it difficult to diagnose OH temporal changes from a single process. The OH source mainly include the primary production from the reaction of excited oxygen atoms ($O(^1D)$) with water vapor (H_2O) and the secondary production mainly from the reaction of nitrogen oxide (NO) or ozone (O_3) with hydroperoxyl radical (HO_2) or organic peroxy radicals (RO_2). The OH sinks mainly include the reaction of OH with carbon monoxide (CO), CH_4, or non-methane volatile organic compounds (NMVOCs).

Based on inversions of *1-1-1 trichloroethane* (methyl chloroform, MCF) atmospheric observations, some previous studies have attributed part of the observed CH_4 changes to the temporal variation in OH

concentrations ([OH]) but report large uncertainties in their estimates (McNorton et al 2016; Rigby et al. 2008, 2017; Turner et al., 2017). Such proxy approaches based on MCF inversions also have limitations in their accuracy, both due to uncertainties in MCF emissions before the 1990s, and the weakening of inter-hemispheric MCF gradients after the 1990s (Krol et al., 2003, Bousquet et al., 2005; Montzka et al., 2011; Prather and Holmes, 2017).

The OH variations have been explored with atmospheric chemistry models in terms of climate change (Nicely et al., 2018), anthropogenic emissions (Gaubert et al. 2017), and lightning NO_x emissions (Murray et al., 2013; Turner et al., 2018). The El Niño-Southern Oscillation (ENSO) has proven to influence [OH] by perturbing CO emissions from biomass burning (Rowlinson et al. 2019) and NO_x emissions from lightning (Turner et al., 2018), but the detailed mechanisms behind present OH variations and their impact on the CH_4 budget remain poorly understood. Nguyen et al. (2020) estimated the impact of the chemical feedback induced by CO and CH_4 changes on the top-down estimates of CH_4 emissions using a box model approach. However, they account neither for the heterogeneous distribution of atmospheric reactive species in space nor for the chemical feedback related to OH production processes that vary over time. Understanding the influences of the chemical feedback related to OH on CH_4 emissions as estimated by atmospheric inversions is urgently needed and can benefit from better incorporating 3D simulations from atmospheric chemistry models.

Here we continue our former studies (Zhao et al., 2019; 2020), in which we have quantified the impact of OH on top-down estimates of CH_4 emissions during the 2000s. This work aims to better understand the production and loss processes of OH and quantitatively assess their influence on the temporal changes of CH_4 lifetime and the global CH_4 budget on decadal-scale since the 1980s. We first analyze the trends and year-to-year variations of nine independent OH fields covering the period of 1980-2010 simulated by the phase 1 of the International Global Atmospheric Chemistry (IGAC)/Stratosphere-troposphere Processes

and their Role in Climate (SPARC) Chemistry-Climate Model Initiative (CCMI) models (Morgenstern et al., 2017) and then assess the contribution of different chemical processes to the OH budget by estimating the main OH production and loss processes. We finally estimate the impact of OH year-to-year variations and trends on the top-down estimation of global CH_4 emissions between 1986 and 2010. Two-box model inversions and the variational 4D inversions are both used to assess how the nonlinear chemical feedback related to OH influences our understanding of the trends and drivers of the global CH_4 budget.

2 Method

2.1 CCMI OH fields

In this study, we analyze the OH fields simulated by five models (CESM1-CAM4Chem, CESM1-WACCM, EMAC-L90MA, GEOSCCM, MRI-ESM1r1), which include detailed tropospheric ozone chemistry and multiple primary VOC emissions. All five models conducted the REF-C1 experiments (free-running simulations driven by state-of-the-art historical forcings including sea surface temperature and sea ice concentrations) for 1960-2010, and four of them (excluding GEOSCCM) conducted the REFC-1SD experiments (similar to REF-C1 but nudged to the reanalysis meteorology data) for 1980-2010. Thus, we have nine OH fields generated by models with different chemistry, physics, and dynamics covering the period 1980-2010. A detailed description of these CCMI models, experiments and characteristics of the OH fields can be found in Morgenstern et al. (2017) and Zhao et al. (2019).

To eliminate the influence of different magnitudes of global OH burden simulated by those models, we scale all OH fields to the same CH_4 loss for the year 2000 based on the reaction with OH used in the TransCom-CH4 inter-comparison exercise (Patra et al., 2011).The inferred global mean scaling factors are calculated for the year 2000 and each OH field and then applied to the whole period (1980-2010). The production ($O(^1D)+H_2O$, $NO+HO_2$, O_3+HO_2) and loss processes (removal of OH by CO, CH_4, formaldehyde (CH_2O), and isoprene) for each OH field are estimated using the CCMI database (Section

S1). For each OH field, we separate trends and year-to-year variations of the global tropospheric mean CH_4 reaction weighted OH concentration ($[OH]_{GM\text{-}CH4}$, weighting factor = reaction rate of OH with CH_4 $\times$ dry air mass, Lawrence et al., 2001) as well as of its production and loss rates.

2.2 Atmospheric inversion systems

To evaluate the influences of OH temporal variations on the top-down estimation of CH_4 emissions, we have conducted Bayesian atmospheric inversions using: 1) a two-box model similar to that described by Turner et al. (2017) and 2) a 4D variational inversion system based on the version LMDz5B of the LMDz atmospheric transport model under the PYVAR-SACS framework (Chevallier et al., 2007; Pison et al., 2009) as described by Locatelli et al. (2015) and Zhao et al. (2020). The two-box model inversions allow us to easily conduct multiple long-term global scale inversions (1984-2012) with each of the nine OH fields to estimate the global CH_4 emission variations caused by various OH fields. The 4D variational inversions allow us to better represent the atmospheric transport, account for the variation of meteorological conditions, and address regional CH_4 emission distributions. Thus, we have conducted both, two-box model inversions with each of the nine OH fields, and variational inversions with the multi-model mean OH field (average of the nine OH fields).

Both the box model and the variational inversions optimize the CH_4 emissions and initial mixing ratios by assimilating the observation data from the Earth System Research Laboratory of the US National Oceanic and Atmospheric Administration (NOAA/ESRL, Dlugokencky et al. (1994)). The OH concentrations are prescribed and not optimized in both inversion systems. A detailed description of the two-box model, the LMDz atmospheric transport model, and the variational inversion method used here are provided in the supplementary material (Section S2).

2.3 Ensemble of different inversions

We have designed an ensemble of inversion experiments as listed in Table 1 using the two-box model with each OH field. Here, Inv_OH_std uses the aforementioned scaled OH fields; Inv_OH_cli uses a climatology of each OH field, which is constant over the years and correspond to an average over 1980-2010; Inv_OH_var stands for the inversion using the detrended OH (only keeping the year-to-year variations); Inv_OH_trend uses the OH without the year-to-year variability (retaining only the trend). By comparing Inv_OH_cli with Inv_OH_std, Inv_OH_var, and Inv_OH_trend, it is possible to assess the influence of total OH temporal changes, year-to-year variations, and OH trends on the overall CH_4 changes, respectively. The box model inversions are conducted from 1984 to 2012 (2010 OH fields are used for 2011 and 2012). The first and last two years are treated as spin-up and spin-down, and we only analyze the inversion results over 1986-2010.

We have conducted two 4D variational inversions, Inv_OH_std and Inv_OH_cli, using the multi-model mean OH field to test the influence of OH temporal variations on the top-down estimates of global to regional CH_4 emissions. The LMDz inversions are conducted for four time periods (1994-1997, 1996-1999, 2000-2004, and 2006-2010; Sect.3.4). We only spin-up/spin-down the 4D variational inversions for one year to save computing time. The four time periods are chosen to represent the transition from La Niña (1995-1996) to El Niño (1997-1998) years and the years of stagnated (2001-2003) and renewed growth (2007-2009) of observed CH_4.

3 Results

3.1 Decadal OH trends and year-to-year variability

All CCMI models simulate positive OH trends from 1980 to 2010 after removing the year-to-year variability (Fig.1, top panel), consistent with previous analyses of CCMI OH fields (Zhao et al., 2019; Nicely et al., 2020) and model results of the Aerosol and Chemistry Model Intercomparison Project

(Stevenson et al., 2020). The multi-model mean $[OH]_{GM\text{-}CH4}$ increased by 0.7×10^5molec cm^{-3} from 1980 to 2010. The growth rates in $[OH]_{GM\text{-}CH4}$ are estimated as ~0.03×10^5molec cm^{-3} yr^{-1} (0.3% yr^{-1}) during the early 1980s, ~0.01×10^5molec cm^{-3} yr^{-1} (0.1% yr^{-1}) between the mid-1980s and the late-1990s, and 0.03-0.05$\times10^5$molec cm^{-3} yr^{-1} (0.3%-0.5% yr^{-1}) since the 2000s. This continuous increases in [OH] is different from the results based on the MCF inversions using the two-box model approach (Turner et al., 2017; Rigby et al., 2017), which yield increases in [OH] from the 1990s to the early 2000s and a decreases in OH afterward.

The ensemble of the anomaly of detrended $[OH]_{GM\text{-}CH4}$ (middle panel of Fig.1) shows a strong anti-correlation (r = -0.50) with the bi-monthly Multivariate ENSO Index Version 2 (MEI, the bottom panel of Fig.1 and Section S3) (Zhang et al., 2019), with higher $[OH]_{GM\text{-}CH4}$ during La Niña and lower $[OH]_{GM\text{-}CH4}$ during El Niño. From 1980 to 2010, the CCMI model simulations show several negative $[OH]_{GM\text{-}CH4}$ anomalies, the three largest reaching as high as $-0.4\pm0.2\times10^5$molec cm^{-3} (-4±2%) during 1982-1983 and 1991-1992, and $-0.5\pm0.4\times10^5$molec cm^{-3} (-5±4%) during 1997-1998. The negative $[OH]_{GM\text{-}CH4}$ anomalies during 1982-1983 and 1997-1998 correspond to the two strongest El Niño events (MEI>2.5). During 1991-1992, the negative $[OH]_{GM\text{-}CH4}$ anomaly corresponds to both, the weaker El Niño event (MEI up to 2.0), and the eruption of Mount Pinatubo. During other weak El Niño events (1986-1987, 2002-2003, 2004-2005, and 2006-2007), the multi-model mean $[OH]_{GM\text{-}CH4}$ shows smaller negative anomalies of 1-2%. Only the negative OH anomaly during 2006-2007 (2±1%) is simulated by all models during the four weak El Niño events. The negative anomalies are consistent with an up to 9% reduction of [OH] during 1997-1998 simulated by TOMCAT-GLOMAP as shown by Rowlinson et al. (2019), as well as a 5% reduction of [OH] over tropical regions during 1991-1993 constrained by MCF observations (Bousquet et al, 2006). During La Niña events, the $[OH]_{GM\text{-}CH4}$ shows ~2% positive anomalies, resulting in more than a 6% increase in OH (max－min) during 1983-1985, 1992-1994, and 1998-2000.

The negative $[OH]_{GM\text{-}CH4}$ anomalies during strong El Niño events correspond to the highest growth rates of the CH_4 mixing ratio from the surface observations (*Dlugokencky, NOAA/ESRL*), which are 14 ± 0.6ppbv yr^{-1} in 1991, and 12 ± 0.8ppbv yr^{-1} in 1998 (Fig.S1). The positive anomalies of $[OH]_{GM\text{-}CH4}$ during La Niña events correspond to a much smaller CH_4 growth (e.g. 4 ± 0.6ppbv yr^{-1} in 1993 and 2 ± 0.8ppbv yr^{-1} in 1999) compared with that during the adjacent El Niño years (Fig. S1).

3.2 Factors controlling OH trends and year-to-year variability

The changes in tropospheric [OH] are due to changes in the balance of production and loss. Here we assess the drivers of OH year-to-year variations and trend by calculating the OH production and loss processes listed in Table 2 following Murray et al. (2013; 2014) and Lelieveld et al. (2016). The multi-model calculated OH production/loss in the troposphere averaged over 1980-2010 is 209 ± 12Tmol yr^{-1}, similar to that ~200Tmol yr^{-1} reported by Murray et al. (2014). Of the total OH production, 46% (96 ± 2Tmol yr^{-1}) are from primary production ($O(^1D) + H_2O$). Two main secondary productions, $NO+HO_2$, and O_3+HO_2 account for 30% (63 ± 4Tmol yr^{-1}) and 13% (26 ± 2Tmol yr^{-1}), respectively. For the OH loss, reactions with CO and CH_4 account for 39% (82 ± 4Tmol yr^{-1}) and 15% (32 ± 1Tmol yr^{-1}), respectively. We have also calculated the OH loss by reactions with isoprene (C_5H_8) and formaldehyde (CH_2O), which both remove 6% of OH, reflecting the influences of NMVOCs from natural and anthropogenic sources, respectively. Besides, there are 12% of OH production and 33% of OH loss not analyzed here due to lack of data in the CCMI model outputs (e.g. output of OH loss due to reaction with NMVOCs included in different models).

Fig.2 shows the changes in the trends of OH production and loss processes (year-to-year variations are removed) with respect to the year 1980. The OH primary production ($O(^1D)+H_2O$) shows a large increase of 10 ± 1Tmol yr^{-1} from 1980 to 2010, as the dominant driver of the positive OH trend. The increase in OH primary production is due to an increase in both tropospheric O_3 burden (producing $O(^1D)$) and water

vapor (Dentener et al 2003; Zhao et al., 2019; Nicely et al., 2020). The OH loss from CO increased by 7 ± 0.7Tmol yr^{-1} from 1980 to 2001 but then decreased by 4 ± 2Tmol yr^{-1} from 2001 to 2010. The negative trend of CO simulated by CCMI models during 2000-2010 is consistent with MOPITT observations over most of the regions (Strode et al., 2016). We find that the decrease in OH loss by CO can explain the accelerated OH increase after 2000, despite a stagnated OH primary production and a slight decrease of the OH secondary production. The OH loss by CH_4, which shows a continuous increase of 6 ± 0.5Tmol yr^{-1} from 1980 to 2010, buffers the increase in OH production by NO (5 ± 1Tmol yr^{-1}). The OH production by O_3+HO_2, as well as OH loss by CH_2O and isoprene, show smaller changes of 2 ± 1Tmol yr^{-1}, 2 ± 0.3Tmol yr^{-1}, and 1 ± 0.6Tmol yr^{-1}, respectively, during 1980-2010. By comparing the magnitude of the production and loss processes, we conclude that an enhanced OH primary production and changes in OH loss by CO are the most important factors leading to the increased OH trend inferred by CCMI models from 1980 to 2010.

Fig.3 and Fig.S2 show the year-to-year variations of the global total OH production and loss due to several processes (calculated after trends have been removed). Year-to-year variations of global [OH] are mainly determined by the primary ($O(^1D)$+H_2O) and secondary production (NO+HO_2; O_3+HO_2) and by OH loss due to CO (Fig.3). Other OH loss processes, including reactions with CH_4, CH_2O, and isoprene, show much smaller year-to-year variations but larger uncertainties (Fig.S2), revealing a larger model spread for these processes.

As shown in Fig.3, negative anomalies of [OH] during El Niño events are dominated by increased OH loss through the reaction with CO in response to enhanced biomass burning (Fig.S3), similar to the conclusions of Rowlinson et al. (2019) and Nicely et al. (2020). During the strong El Niño events in 1982-1983, 1991-1992, and 1997-1998, the OH loss by CO increased by up to 3 ± 0.4Tmol yr^{-1}, 5 ± 0.6Tmol yr^{-1}, and 8 ± 0.5Tmol yr^{-1}, respectively, compared to the mean value of 1980-2010. The increase of OH loss

by CO can be partly offset by an increase in OH production. Indeed, in 1998, the OH primary production ($O(^1D)+H_2O$), OH produced by $NO+RO_2$, and O_3+RO_2 increased by 3 ± 0.7Tmol yr^{-1}, 3 ± 0.5Tmol yr^{-1}, and 2 ± 0.3Tmol yr^{-1}, respectively, offsetting most of the OH loss increase. The increase in OH primary production is mainly due to an increase in tropospheric water vapor and O_3 burden during El Niño events (Fig.S3 and S12 in Nicely et al. (2020)), while the increase in OH secondary production is caused by enhanced NO_x emissions (Fig.S3) and O_3 formation (Nicely et al. (2020) related to biomass burning as well as more HO_2 formation by CO+OH. As a result, the OH year-to-year variations found here are much smaller than those estimated by Nguyen et al. (2020), who mainly considered the response of OH to enhanced CO emissions during the El Niño events. The positive anomaly in OH primary production (0.2 ± 0.5Tmol yr^{-1}) is not significant during the 1991-1992 El Niño event, maybe due to absorption of ultraviolet (UV) by volcanic SO_2 and scattering of UV by sulfate aerosols as well as reduction of tropospheric water vapor after the eruption of Mount Pinatubo (Bândă et al., 2016; Soden et al., 2020). Thus, the negative [OH] anomaly during the weak El Niño event in 1991-1992 is potentially being enhanced by the eruption of Mount Pinatubo. Previous studies have shown that NO_x emissions from lightning can contribute to the OH interannual variability (Murray et al., 2013; Turner et al. 2018). In addition, soil NO_x emissions depend on temperature and soil humidity (Yienger and Levy, 1995), which vary during the El Niño events. The year-to-year variations of NO_x emissions from lightning show large differences among CCMI models (Fig. S4), and only EMAC and GEOSCCM apply interactive soil NO_x emissions that vary with meteorology conditions (Morgenstern et al., 2017) based on Yienger and Levy (1995). Thus NO_x emissions from lightning and soil mainly contribute to inter-model differences instead of showing a consistent response to El Niño.

Using a machine learning method, Nicely et al. (2020) attributed the positive [OH] trend simulated by the CCMI models mainly to the increase of tropospheric O_3, $J(O^1D)$, NO_x and H_2O, and attributed [OH] interannual variations to CO changes. Overall, the explanations of the drivers of OH year-to-year

variations and trends found in our process analysis are broadly consistent with those reported by Nicely et al. (2020), and we emphasize that the decrease of CO emission and concentrations after 2000 (Zheng et al., 2019) is important for determining the accelerated positive OH trend.

3.3 Impact of OH variation on the top-down estimation of CH_4 budget

Fig.4a shows the anomaly of global total CH_4 emission estimated by inv_OH_std (nine scaled OH fields; yellow line) and inv_OH_cli (nine climatological OH; blue line) using the two-box model during 1986-2010. With the climatological OH fields (blue line), the top-down estimated CH_4 emissions show no clear trend before 2005, with large positive anomalies during strong El Niño years. There are two peaks of positive CH_4 emission anomalies during this period, 10Tg yr^{-1} in 1991, and 14Tg yr^{-1} in 1998. From 2005 to 2008, the CH_4 emissions show a large increase of 26Tg yr^{-1}. The CH_4 emissions averaged over 2006-2010 is 20Tg yr^{-1} higher than over 2000-2005, consistent with 17–22Tg yr^{-1} estimated by an ensemble of inversions in Kirschke et al. (2013).

The OH temporal variations are found to largely influence the interannual changes of top-down estimated CH_4 emissions (yellow line of Fig. 4a), with differences between the two inversions reaching up to more than 15Tg yr^{-1} (Fig.4b). The contribution from the OH year-to-year variations and trends are also shown in Fig.4. The negative anomalies of OH during El Niño years reduce the unusually high top-down estimated CH_4 emissions in 1991-1992 by 7±3Tg yr^{-1}, and in 1998 by 10±3Tg yr^{-1} (Fig.4c). As a result, the high emission peaks to match the observed CH_4 mixing ratio growth in 1991 (14ppb yr^{-1}) and 1998 (12ppbv yr^{-1}), as estimated using the climatological OH are largely reduced.

The identified positive OH trend leads to an additional 23±9Tg yr^{-1} increase in CH_4 emissions from 1986 to 2010 (Fig.4d). During 1986-2005, the mean CH_4 emissions, as estimated with the scaled OH, show a positive trend of 0.6±0.4Tg yr^{-2} ($P<0.05$). Increased CH_4 emissions offset the increase in the OH sink to

match the observations. From 2005 to 2008, in contrast to previous studies, which attribute the increased observed CH_4 mixing ratios to decreased OH based on MCF inversions (Turner et al., 2017, Rigby et al., 2017), the increasing OH trend simulated by CCMI models results in an additional 5±2Tg yr^{-1} CH_4 emission increase in the inversion to match the observations.

We compare the inversion using the two-box model ("**x**" in Fig.5) with the results from the variational approach (bars in Fig.5), using the multi-model mean OH field, to evaluate the performance of the simplified two-box model inversions. Despite the limitations inherent to two-box model inversions, such as treatment of inter-hemispheric transport, stratospheric loss, and the impact of spatial variability (Naus et al., 2019), the two-box model inversion estimates similar temporal changes of CH_4 emissions and losses compare to the variational approach for the four periods, as well as their response to OH changes (Fig.5), on a global scale. Such comparisons reinforce the reliability of the conclusions made from the two-box model inversions regarding changes in the global total CH_4 budget.

The variational inversions allow us to assess the regional contribution of the drivers to observed atmospheric CH_4 mixing ratio changes. Here, as a synthesis, we focus on four latitude bands (Fig.5 and Table S2), including the southern extra-tropical regions (90 °S-30 °S), the tropical regions (30 °S-30 °N), and the northern temperate (30 °-60 °N) and boreal (60 °-90 °N) regions. On average, OH over the tropical and northern temperate regions removes 74% and 14% of global total atmospheric CH_4, respectively.

Between the periods 1995-1996 and 1997-1998, if one does not consider the OH temporal variations (Inv_OH_cli), the CH_4 loss by OH shows a slight increase of 2Tg yr^{-1} due to an increase of atmospheric CH_4 mixing ratios. The main driver of observed atmospheric CH_4 mixing ratio changes is the 10Tg yr^{-1} increase of CH_4 emission over the Tropics and the 7Tg yr^{-1} increase over the northern temperate regions (middle panel of Fig.5 and Table S2). When the multi-model mean OH temporal variations are included

(Inv_OH_std), the negative anomaly of OH in 1997-1998 led to a 9Tg yr^{-1} decrease in CH_4 loss in 1997-1998 compared to 1995-1996, of which 7Tg y^{-1} (78%) are contributed by the tropical regions (left panel of Fig.5). As a result, the decrease of CH_4 loss by OH contributes a bit more to match the observed CH_4 mixing ratios increase during the El Niño periods than the changes in CH_4 emissions (a global increase of 8Tg yr^{-1}). The emission increases from 1995-1996 to 1997-1998 over the Tropics and the northern temperate regions are reduced to 3Tg yr^{-1} and 5Tg yr^{-1} (left panel of Fig.5, Inv_OH_std), respectively, similar to the inversion results given by Bousquet et al. (2006).

From the period 2001-2003 to 2007-2009, positive OH trends lead to a 13Tg yr^{-1} increase of the CH_4 loss, of which 10Tg yr^{-1} (76%) originates from the Tropics (Inv_OH_std, left panel of Fig.5). In response to increased CH_4 losses, the increase of optimized emissions over tropical regions (16Tg yr^{-1}, Inv_OH_std) is more than twice that of the inversion using climatological OH (7Tg yr^{-1}, Inv_OH_cli). The emission increases during the two periods over the northern region show a smaller change of 2Tg yr^{-1} (12 Tg yr^{-1} estimated by Inv_OH_std versus 10 Tg yr^{-1} by Inv_OH_cli, Fig. 5). The variational inversions show that the OH temporal variations are most critical for top-down estimates of CH_4 budgets over the tropical regions since OH over tropical regions shows larger interannual variations and trend than mid to high latitude regions (Fig.S5) and most of the CH_4 (74%) is removed from the atmosphere by OH over the tropical regions.

4 Conclusion and discussion

Based on the simulations from the CCMI, we explore the response of OH fields to changes in climate, anthropogenic and natural emissions and their impact on the top-down estimates of CH_4 emissions during 1980-2010 based on a model perspective. We find that although CCMI models simulated rather different global total burdens of OH (Zhao et al., 2019), they show very similar patterns in temporal variations, including (1) negative anomalies during El Niño years, which are mainly driven by an elevated OH loss

by reaction with CO from enhanced biomass burning, despite a partial buffering through enhanced OH production, and (2) a continuous increasing in OH from 1980, which is mostly contributed by OH primary production and accelerating after 2000 due to reduced CO emissions. By conducting inversions using a two-box model and a variational approach together with the ensemble of CCMI OH fields, we find that (1) the OH year-to-year variations can largely reduce the CH_4 emission increase (by up to 10Tg yr^{-1}) needed to match the observed CH_4 increase during El Niño years, and (2) the positive OH trend results in 23 ± 9Tg yr^{-1} additional increase in optimized emissions from 1986 to 2010 compared to the inversions using constant OH. The variational inversions also show that OH temporal variations mainly influence top-down estimates of CH_4 emissions over tropical regions.

The responses of OH to changes in biomass burning, ozone, water vapor, and lightning NO_x emissions during El Niño years have been recognized by previous studies (Holmes et al., 2013; Murray et al., 2014; Turner et al., 2018; Rowlinson et al., 2019; Nguyen et al., 2020). Here, the consistent temporal variations of CCMI OH fields increase our confidence in the model simulated response of OH to ENSO as a result of several nonlinear chemical processes. We estimated that the negative OH anomaly in 1998 reduces the high top-down estimated CH_4 emissions by 10 ± 3Tg yr^{-1}, ~40% smaller than the reduction estimated by Butler et al. (2005) (16Tg yr^{-1}), which only include the OH reduction response to enhanced biomass burning CO emissions. The smaller CH_4 emission reduction (OH anomaly) estimated with CCMI OH fields may reflect the significance of considering multi chemical processes as included in the 3D atmospheric chemistry model in capturing OH variations and inverting for CH_4 emissions. One of the largest uncertainties is NO_x emissions from lightning, which have been proven to contribute to year-to-year variations in OH (Murray et al., 2013; Turner et al., 2018), but here show a large spread among CCMI models. In addition, NO_x emissions from soil may also change during El Niño years. Improving estimates of NO_x emissions from lightning based on satellite observations (Murray et al., 2013) and a better representation of the interactive NO_x emissions from the soil are critical for improving the model

simulation of OH temporal variability and for top-down estimates of year-to-year variations of CH_4 emissions.

The positive trend of OH after the mid-2000s, which results in enhanced top-down estimated CH_4 emissions over the Tropics, is opposite to those constrained by MCF inversions (Turner et al., 2017; Rigby et al., 2017). The processes that control the model simulated positive OH trend discussed in this study are supported by current studies based on observations, including decreased CO emissions (Zheng et al., 2019), small variations of global NO_x emissions (Miyazaki et al., 2017), and an increase in tropospheric ozone (Ziemke et al., 2019) and water vapor (Chung et al., 2014). However, the CCMI models still show biases that are related to OH production and loss. For example, these include an underestimation of CO especially over the northern hemisphere compared with the surface and satellite observations (Naik et al., 2013; Strode et al., 2016) and bias in atmospheric total O_3 column (Zhao et al. 2019). In addition, changes in aerosols (Tang et al., 2003) and atmospheric circulation such as the Hadley cell expansion (Nicely et al., 2018) are not discussed in this study. Given the uncertainties in both atmospheric chemistry model simulated (Naik et al., 2013; Zhao et al., 2019) and MCF-constrained OH (Bousquet et al., 2005; Prather and Holmes, 2017; Naus et al. et al., 2019), and the large discrepancy between the two methods, the OH trend after the mid-2000s remains an open problem and more effort is required in both methods to close the gap.

The temporal variations of OH, which are generally not well constrained in current top-down estimates of CH_4 emissions, imply potential additional uncertainties in the global CH_4 budget (Saunois et al., 2017; Zhao et al., 2020). The tropical regions, where top-down estimated CH_4 emissions show the largest sensitivity to OH changes, represent more than 60% of CH_4 emissions worldwide (Saunois et al., 2016). The tropical CH_4 emissions are dominated by wetland emissions, of which large uncertainties exist in both bottom-up and top-down studies (Saunois et al., 2016; 2017). The variational inversions using OH

with temporal variations attribute the observed rising CH_4 growth during El Niño to the reduction of CH_4 loss instead of enhanced emissions over the Tropics, which are consistent with process-based wetland models that estimated wetland CH_4 emission reductions at beginning of El Niño event (Hodson et al., 2011; Zhang et al., 2018). Also, the negative OH anomaly can reduce the top-down estimated biomass burning CH_4 emission spikes during El Niño events, consistent with that given by Bousquet et al. (2006). Future climate projections show that the extreme El Niño events will be more frequent under a warmer climate (Berner et al., 2020), which may enhance the fluctuations in [OH]. Furthermore, the changes in anthropogenic emissions, e.g. such as expected decreases in NO_x emissions (Lamarque et al., 2013), can also affect the OH trends. Our research emphasizes the importance of considering climate changes and chemical feedbacks related to OH in future CH_4 budget research.

Data availability

The CCMI OH fields are available at the Centre for Environmental Data Analysis (CEDA; http://data.ceda.ac.uk/badc/wcrp-ccmi/data/CCMI-1/output; Hegglin and Lamarque, 2015), the Natural Environment Research Council's Data Repository for Atmospheric Science and Earth Observation. The CESM1-WACCM outputs for CCMI are available at http://www.earthsystemgrid.org (Climate Data Gateway at NCAR, 2019). The surface observations for CH_4 inversions are available at the World Data Centre for Greenhouse Gases (WDCGG, https://gaw.kishou.go.jp/, 2019). Other datasets can be accessed by contacting the corresponding author.

Author contributions

YZ, BZ, MS, and PB designed the study, analyzed data and wrote the manuscript. AB developed the LMDz code for variational CH_4 inversions. XL helped with data preparation. JC and RJ provided input into the study design and discussed the results. ED provided the atmospheric in situ data. MH, MD, PJ, DK, OK, SS, and ST provided CCMI model outputs. All co-authors commented on the manuscript.

Acknowledgements

This work benefited from the expertise of the Global Carbon Project methane initiative.

We acknowledge the modeling groups for making their simulations available for this analysis, the joint WCRP SPARC/IGAC Chemistry–Climate Model Initiative (CCMI) for organizing and coordinating the model simulations and data analysis activity, and the British Atmospheric Data Centre (BADC) for collecting and archiving the CCMI model output.

The EMAC model simulations have been performed at the German Climate Computing Centre (DKRZ) through support from the Bundesministerium für Bildung und Forschung (BMBF). DKRZ and its scientific steering committee are gratefully acknowledged for providing the HPC and data archiving resources for the consortial project ESCiMo (Earth System Chemistry integrated Modelling).

Makoto Deushi was partly supported by JSPS KAKENHI grant no. JP19K12312.

Yuanhong Zhao acknowledges helpful discussions with Zhen Zhang, Yilong Wang, and Lin Zhang.

Competing interests

The authors declare that they have no conflicts of interest.

Financial support

This research has been supported by the Gordon and Betty Moore Foundation (grant no. GBMF5439), "Advancing Understanding of the Global Methane Cycle".

Reference

Bândă, N., Krol, M., van Weele, M., van Noije, T., Le Sager, P., and Röckmann, T.: Can we explain the observed methane variability after the Mount Pinatubo eruption?, Atmos. Chem. Phys., 16, 195-214, 10.5194/acp-16-195-2016, 2016.

Berner, J., Christensen, H. M., and Sardeshmukh, P. D.: Does ENSO Regularity Increase in a Warming Climate?, Journal of Climate, 33, 1247-1259, 10.1175/jcli-d-19-0545.1, 2020.

Bousquet, P., Hauglustaine, D. A., Peylin, P., Carouge, C., and Ciais, P.: Two decades of OH variability as inferred by an inversion of atmospheric transport and chemistry of methyl chloroform, Atmos. Chem. Phys., 5, 2635-2656, 10.5194/acp-5-2635-2005, 2005.

Bousquet, P., Ciais, P., Miller, J. B., Dlugokencky, E. J., Hauglustaine, D. A., Prigent, C., Van der Werf, G. R., Peylin, P., Brunke, E. G., Carouge, C., Langenfelds, R. L., Lathiere, J., Papa, F., Ramonet, M., Schmidt, M., Steele, L. P., Tyler, S. C., and White, J.: Contribution of anthropogenic and natural sources to atmospheric methane variability, Nature, 443, 439-443, 10.1038/nature05132, 2006.

Chevallier, F., Bréon, F.-M., and Rayner, P. J.: Contribution of the Orbiting Carbon Observatory to the estimation of CO2 sources and sinks: Theoretical study in a variational data assimilation framework, Journal of Geophysical Research: Atmospheres, 112, 10.1029/2006jd007375, 2007.

Chung, E.-S., Soden, B., Sohn, B. J., and Shi, L.: Upper-tropospheric moistening in response to anthropogenic warming, Proceedings of the National Academy of Sciences, 111, 11636-11641, 10.1073/pnas.1409659111, 2014.

Dentener, F., Peters, W., Krol, M., van Weele, M., Bergamaschi, P., and Lelieveld, J.: Interannual variability and trend of CH4 lifetime as a measure for OH changes in the 1979–1993 time period, Journal of Geophysical Research: Atmospheres, 108, 4442, 10.1029/2002jd002916, 2003.

Dlugokencky, E., Steele, L., Lang, P., and Masarie, K.: The growth rate and distribution of atmospheric methane, Journal of Geophysical Research: Atmospheres, 99, 17021-17043, 1994.

Dlugokencky, NOAA/ESRL ,www.esrl.noaa.gov/gmd/ccgg/trends_ch4/, 2020

Etheridge, D. M., Steele, L. P., Francey, R. J., and Langenfelds, R. L.: Atmospheric methane between 1000 A.D. and present: Evidence of anthropogenic emissions and climatic variability, Journal of Geophysical Research: Atmospheres, 103, 15979-15993, 10.1029/98jd00923, 1998.

Etminan, M., Myhre, G., Highwood, E. J., and Shine, K. P.: Radiative forcing of carbon dioxide, methane, and nitrous oxide: A significant revision of the methane radiative forcing, Geophysical Research Letters, 43, 12,614-612,623, doi:10.1002/2016GL071930, 2016.

Gaubert, B., Worden, H. M., Arellano, A. F. J., Emmons, L. K., Tilmes, S., Barré, J., Martinez Alonso, S., Vitt, F., Anderson, J. L., Alkemade, F., Houweling, S., and Edwards, D. P.: Chemical Feedback From Decreasing Carbon Monoxide Emissions, Geophysical Research Letters, 44, 9985-9995, 10.1002/2017gl074987, 2017.

Hegglin, M. I. and Lamarque, J.-F.: The IGAC/SPARC Chemistry-Climate Model Initiative Phase-1 (CCMI-1) model data output, NCAS British Atmospheric Data Centre, [ADD ACCESS DATE], available at: http://catalogue.ceda.ac.uk/uuid/ 9cc6b94df0f4469d8066d69b5df879d5, 2015.

Hodson, E. L., Poulter, B., Zimmermann, N. E., Prigent, C., and Kaplan, J. O.: The El Niño–Southern Oscillation and wetland methane interannual variability, Geophysical Research Letters, 38, 10.1029/2011gl046861, 2011.

Holmes, C. D., Prather, M. J., Søvde, O. A., and Myhre, G.: Future methane, hydroxyl, and their uncertainties: key climate and emission parameters for future predictions, Atmospheric Chemistry and Physics, 13, 285-302, 10.5194/acp-13-285-2013, 2013.

Kirschke, S., Bousquet, P., Ciais, P., Saunois, M., Canadell, J. G., Dlugokencky, E. J., Bergamaschi, P., Bergmann, D., Blake, D. R., Bruhwiler, L., Cameron-Smith, P., Castaldi, S., Chevallier, F., Feng, L., Fraser, A., Heimann, M., Hodson, E. L., Houweling, S., Josse, B., Fraser, P. J., Krummel, P. B., Lamarque, J.-F., Langenfelds, R. L., Le Quéré, C., Naik, V., O'Doherty, S., Palmer, P. I., Pison, I., Plummer, D., Poulter, B., Prinn, R. G., Rigby, M., Ringeval, B., Santini, M., Schmidt, M., Shindell, D. T., Simpson, I. J., Spahni, R., Steele, L. P., Strode, S. A., Sudo, K., Szopa, S., van der Werf, G. R., Voulgarakis, A., van

Weele, M., Weiss, R. F., Williams, J. E., and Zeng, G.: Three decades of global methane sources and sinks, Nature Geoscience, 6, 813-823, https://doi.org/10.1038/ngeo1955, 2013.

Krol, M. C., Lelieveld, J., Oram, D. E., Sturrock, G. A., Penkett, S. A., Brenninkmeijer, C. A. M., Gros, V., Williams, J., and Scheeren, H. A.: Continuing emissions of methyl chloroform from Europe, Nature, 421, 131-135, 10.1038/nature01311, 2003.

Lamarque, J. F., Shindell, D. T., Josse, B., Young, P. J., Cionni, I., Eyring, V., Bergmann, D., Cameron-Smith, P., Collins, W. J., Doherty, R., Dalsoren, S., Faluvegi, G., Folberth, G., Ghan, S. J., Horowitz, L. W., Lee, Y. H., MacKenzie, I. A., Nagashima, T., Naik, V., Plummer, D., Righi, M., Rumbold, S. T., Schulz, M., Skeie, R. B., Stevenson, D. S., Strode, S., Sudo, K., Szopa, S., Voulgarakis, A., and Zeng, G.: The Atmospheric Chemistry and Climate Model Intercomparison Project (ACCMIP): overview and description of models, simulations and climate diagnostics, Geoscientific Model Development, 6, 179-206, 10.5194/gmd-6-179-2013, 2013.

Lawrence, M. G., Jöckel, P., and von Kuhlmann, R.: What does the global mean OH concentration tell us?, Atmos. Chem. Phys., 1, 37-49, 10.5194/acp-1-37-2001, 2001.

Lelieveld, J., Gromov, S., Pozzer, A., and Taraborrelli, D.: Global tropospheric hydroxyl distribution, budget and reactivity, Atmos. Chem. Phys., 16, 12477-12493, 10.5194/acp-16-12477-2016, 2016.

Locatelli, R., Bousquet, P., Hourdin, F., Saunois, M., Cozic, A., Couvreux, F., Grandpeix, J. Y., Lefebvre, M. P., Rio, C., Bergamaschi, P., Chambers, S. D., Karstens, U., Kazan, V., van der Laan, S., Meijer, H. A. J., Moncrieff, J., Ramonet, M., Scheeren, H. A., Schlosser, C., Schmidt, M., Vermeulen, A., and Williams, A. G.: Atmospheric transport and chemistry of trace gases in LMDz5B: evaluation and implications for inverse modelling, Geosci. Model Dev., 8, 129-150, 10.5194/gmd-8-129-2015, 2015.

McNorton, J., Chipperfield, M. P., Gloor, M., Wilson, C., Feng, W., Hayman, G. D., Rigby, M., Krummel, P. B., amp, apos, Doherty, S., Prinn, R. G., Weiss, R. F., Young, D., Dlugokencky, E., and Montzka, S. A.: Role of OH variability in the stalling of the global atmospheric CH₄ growth rate from 1999 to 2006, Atmospheric Chemistry and Physics, 16, 7943-7956, 10.5194/acp-16-7943-2016, 2016.

Miyazaki, K., Eskes, H., Sudo, K., Boersma, K. F., Bowman, K., and Kanaya, Y.: Decadal changes in global surface NOx emissions from multi-constituent satellite data assimilation, Atmos. Chem. Phys., 17, 807-837, 10.5194/acp-17-807-2017, 2017.

Montzka, S. A., Krol, M., Dlugokencky, E., Hall, B., Jöckel, P., and Lelieveld, J.: Small Interannual Variability of Global Atmospheric Hydroxyl, Science, 331, 67-69, 10.1126/science.1197640, 2011.

Morgenstern, O., Hegglin, M. I., Rozanov, E., amp, apos, Connor, F. M., Abraham, N. L., Akiyoshi, H., Archibald, A. T., Bekki, S., Butchart, N., Chipperfield, M. P., Deushi, M., Dhomse, S. S., Garcia, R. R., Hardiman, S. C., Horowitz, L. W., Jöckel, P., Josse, B., Kinnison, D., Lin, M., Mancini, E., Manyin, M. E., Marchand, M., Marécal, V., Michou, M., Oman, L. D., Pitari, G., Plummer, D. A., Revell, L. E., Saint-Martin, D., Schofield, R., Stenke, A., Stone, K., Sudo, K., Tanaka, T. Y., Tilmes, S., Yamashita, Y., Yoshida, K., and Zeng, G.: Review of the global models used within phase 1 of the Chemistry–Climate

Model Initiative (CCMI), Geoscientific Model Development, 10, 639-671, 10.5194/gmd-10-639-2017, 2017.

Multivariate ENSO Index Version 2，available at https://www.esrl.noaa.gov/psd/enso/mei/ , 2020

Murray, L. T., Logan, J. A., and Jacob, D. J.: Interannual variability in tropical tropospheric ozone and OH: The role of lightning, Journal of Geophysical Research: Atmospheres, 118, 11,468-411,480, 10.1002/jgrd.50857, 2013.

Murray, L. T., Mickley, L. J., Kaplan, J. O., Sofen, E. D., Pfeiffer, M., and Alexander, B.: Factors controlling variability in the oxidative capacity of the troposphere since the Last Glacial Maximum, Atmospheric Chemistry and Physics, 14, 3589-3622, 10.5194/acp-14-3589-2014, 2014.

Naus, S., Montzka, S. A., Pandey, S., Basu, S., Dlugokencky, E. J., and Krol, M.: Constraints and biases in a tropospheric two-box model of OH, Atmos. Chem. Phys., 19, 407-424, 10.5194/acp-19-407-2019, 2019.

Nguyen, N. H., Turner, A. J., Yin, Y., Prather, M. J., and Frankenberg, C.: Effects of Chemical Feedbacks on Decadal Methane Emissions Estimates, Geophysical Research Letters, 47, e2019GL085706, 10.1029/2019gl085706, 2020.

Nicely, J. M., Canty, T. P., Manyin, M., Oman, L. D., Salawitch, R. J., Steenrod, S. D., Strahan, S. E., and Strode, S. A.: Changes in Global Tropospheric OH Expected as a Result of Climate Change Over the Last Several Decades, Journal of Geophysical Research: Atmospheres, 123, 10,774-710,795, doi:10.1029/2018JD028388, 2018.

Nicely, J. M., Duncan, B. N., Hanisco, T. F., Wolfe, G. M., Salawitch, R. J., Deushi, M., Haslerud, A. S., Jöckel, P., Josse, B., Kinnison, D. E., Klekociuk, A., Manyin, M. E., Marécal, V., Morgenstern, O., Murray, L. T., Myhre, G., Oman, L. D., Pitari, G., Pozzer, A., Quaglia, I., Revell, L. E., Rozanov, E., Stenke, A., Stone, K., Strahan, S., Tilmes, S., Tost, H., Westervelt, D. M., and Zeng, G.: A machine learning examination of hydroxyl radical differences among model simulations for CCMI-1, Atmos. Chem. Phys., 20, 1341-1361, 10.5194/acp-20-1341-2020, 2020.

Soden, B. J., Wetherald, R. T., Stenchikov, G. L., and Robock, A.: Global Cooling After the Eruption of Mount Pinatubo: A Test of Climate Feedback by Water Vapor, Science, 296, 727-730, 10.1126/science.296.5568.727, 2002.

Stevenson, D. S., Zhao, A., Naik, V., O'Connor, F. M., Tilmes, S., Zeng, G., Murray, L. T., Collins, W. J., Griffiths, P., Shim, S., Horowitz, L. W., Sentman, L., and Emmons, L.: Trends in global tropospheric hydroxyl radical and methane lifetime since 1850 from AerChemMIP, Atmos. Chem. Phys. Discuss., 2020, 1-25, 10.5194/acp-2019-1219, 2020.

Patra, P. K., Houweling, S., Krol, M., Bousquet, P., Belikov, D., Bergmann, D., Bian, H., Cameron-Smith, P., Chipperfield, M. P., Corbin, K., Fortems-Cheiney, A., Fraser, A., Gloor, E., Hess, P., Ito, A., Kawa, S. R., Law, R. M., Loh, Z., Maksyutov, S., Meng, L., Palmer, P. I., Prinn, R. G., Rigby, M., Saito, R., and Wilson, C.: TransCom model simulations of CH4 and related species: linking transport, surface flux and chemical loss with CH4 variability in the troposphere and lower stratosphere, Atmospheric Chemistry

and Physics, 11, 12813-12837, 10.5194/acp-11-12813-2011, 2011.
Pison, I., Bousquet, P., Chevallier, F., Szopa, S., and Hauglustaine, D.: Multi-species inversion of CH4, CO and H2 emissions from surface measurements, Atmos. Chem. Phys., 9, 5281-5297, 10.5194/acp-9-5281-2009, 2009.
Prather, M. J., and Holmes, C. D.: Overexplaining or underexplaining methane's role in climate change, Proceedings of the National Academy of Sciences, 114, 5324-5326, 10.1073/pnas.1704884114, 2017.
Rigby, M., Prinn, R. G., Fraser, P. J., Simmonds, P. G., Langenfelds, R. L., Huang, J., Cunnold, D. M., Steele, L. P., Krummel, P. B., Weiss, R. F., O'Doherty, S., Salameh, P. K., Wang, H. J., Harth, C. M., Mühle, J., and Porter, L. W.: Renewed growth of atmospheric methane, Geophysical Research Letters, 35, L22805, 10.1029/2008gl036037, 2008.
Rigby, M., Montzka, S. A., Prinn, R. G., White, J. W. C., Young, D., O'Doherty, S., Lunt, M. F., Ganesan, A. L., Manning, A. J., Simmonds, P. G., Salameh, P. K., Harth, C. M., Muhle, J., Weiss, R. F., Fraser, P. J., Steele, L. P., Krummel, P. B., McCulloch, A., and Park, S.: Role of atmospheric oxidation in recent methane growth, Proc Natl Acad Sci U S A, 114, 5373-5377, 10.1073/pnas.1616426114, 2017.
Rowlinson, M. J., Rap, A., Arnold, S. R., Pope, R. J., Chipperfield, M. P., McNorton, J., Forster, P., Gordon, H., Pringle, K. J., Feng, W., Kerridge, B. J., Latter, B. L., and Siddans, R.: Impact of El Niño–Southern Oscillation on the interannual variability of methane and tropospheric ozone, Atmos. Chem. Phys., 19, 8669-8686, 10.5194/acp-19-8669-2019, 2019.
Saunois, M., Bousquet, P., Poulter, B., Peregon, A., Ciais, P., Canadell, J. G., Dlugokencky, E. J., Etiope, G., Bastviken, D., Houweling, S., Janssens-Maenhout, G., Tubiello, F. N., Castaldi, S., Jackson, R. B., Alexe, M., Arora, V. K., Beerling, D. J., Bergamaschi, P., Blake, D. R., Brailsford, G., Brovkin, V., Bruhwiler, L., Crevoisier, C., Crill, P., Covey, K., Curry, C., Frankenberg, C., Gedney, N., Höglund-Isaksson, L., Ishizawa, M., Ito, A., Joos, F., Kim, H. S., Kleinen, T., Krummel, P., Lamarque, J. F., Langenfelds, R., Locatelli, R., Machida, T., Maksyutov, S., McDonald, K. C., Marshall, J., Melton, J. R., Morino, I., Naik, V., O'Doherty, S., Parmentier, F. J. W., Patra, P. K., Peng, C., Peng, S., Peters, G. P., Pison, I., Prigent, C., Prinn, R., Ramonet, M., Riley, W. J., Saito, M., Santini, M., Schroeder, R., Simpson, I. J., Spahni, R., Steele, P., Takizawa, A., Thornton, B. F., Tian, H., Tohjima, Y., Viovy, N., Voulgarakis, A., van Weele, M., van der Werf, G. R., Weiss, R., Wiedinmyer, C., Wilton, D. J., Wiltshire, A., Worthy, D., Wunch, D., Xu, X., Yoshida, Y., Zhang, B., Zhang, Z., and Zhu, Q.: The global methane budget 2000–2012, Earth Syst. Sci. Data, 8, 697-751, 10.5194/essd-8-697-2016, 2016.
Saunois, M., Bousquet, P., Poulter, B., Peregon, A., Ciais, P., Canadell, J. G., Dlugokencky, E. J., Etiope, G., Bastviken, D., Houweling, S., Janssens-Maenhout, G., Tubiello, F. N., Castaldi, S., Jackson, R. B., Alexe, M., Arora, V. K., Beerling, D. J., Bergamaschi, P., Blake, D. R., Brailsford, G., Bruhwiler, L., Crevoisier, C., Crill, P., Covey, K., Frankenberg, C., Gedney, N., Höglund-Isaksson, L., Ishizawa, M., Ito, A., Joos, F., Kim, H. S., Kleinen, T., Krummel, P., Lamarque, J. F., Langenfelds, R., Locatelli, R., Machida, T., Maksyutov, S., Melton, J. R., Morino, I., Naik, V., O'Doherty, S., Parmentier, F. J. W., Patra, P. K., Peng, C., Peng, S., Peters, G. P., Pison, I., Prinn, R., Ramonet, M., Riley, W. J., Saito, M., Santini, M.,

Schroeder, R., Simpson, I. J., Spahni, R., Takizawa, A., Thornton, B. F., Tian, H., Tohjima, Y., Viovy, N., Voulgarakis, A., Weiss, R., Wilton, D. J., Wiltshire, A., Worthy, D., Wunch, D., Xu, X., Yoshida, Y., Zhang, B., Zhang, Z., and Zhu, Q.: Variability and quasi-decadal changes in the methane budget over the period 2000–2012, Atmos. Chem. Phys., 17, 11135-11161, 10.5194/acp-17-11135-2017, 2017.

Saunois, M., Stavert, A. R., Poulter, B., Bousquet, P., Canadell, J. G., Jackson, R. B., Raymond, P. A., Dlugokencky, E. J., Houweling, S., Patra, P. K., Ciais, P., Arora, V. K., Bastviken, D., Bergamaschi, P., Blake, D. R., Brailsford, G., Bruhwiler, L., Carlson, K. M., Carrol, M., Castaldi, S., Chandra, N., Crevoisier, C., Crill, P. M., Covey, K., Curry, C. L., Etiope, G., Frankenberg, C., Gedney, N., Hegglin, M. I., Höglund-Isakson, L., Hugelius, G., Ishizawa, M., Ito, A., Janssens-Maenhout, G., Jensen, K. M., Joos, F., Kleinen, T., Krummel, P. B., Langenfelds, R. L., Laruelle, G. G., Liu, L., Machida, T., Maksyutov, S., McDonald, K. C., McNorton, J., Miller, P. A., Melton, J. R., Morino, I., Müller, J., Murgia-Flores, F., Naik, V., Niwa, Y., Noce, S., O'Doherty, S., Parker, R. J., Peng, C., Peng, S., Peters, G. P., Prigent, C., Prinn, R., Ramonet, M., Regnier, P., Riley, W. J., Rosentreter, J. A., Segers, A., Simpson, I. J., Shi, H., Smith, S. J., Steele, L. P., Thornton, B. F., Tian, H., Tohjima, Y., Tubiello, F. N., Tsuruta, A., Viovy, N., Voulgarakis, A., Weber, T. S., van Weele, M., van der Werf, G. R., Weiss, R. F., Worthy, D., Wunch, D., Yin, Y., Yoshida, Y., Zhang, W., Zhang, Z., Zhao, Y., Zheng, B., Zhu, Q., Zhu, Q., and Zhuang, Q.: The Global Methane Budget 2000-2017, Earth Syst. Sci. Data Discuss., 2019, 1-136, 10.5194/essd-2019-128, 2019.

Strode, S. A., Worden, H. M., Damon, M., Douglass, A. R., Duncan, B. N., Emmons, L. K., Lamarque, J. F., Manyin, M., Oman, L. D., Rodriguez, J. M., Strahan, S. E., and Tilmes, S.: Interpreting space-based trends in carbon monoxide with multiple models, Atmos. Chem. Phys., 16, 7285-7294, 10.5194/acp-16-7285-2016, 2016.

Tang, Y., Carmichael, G. R., Uno, I., Woo, J.-H., Kurata, G., Lefer, B., Shetter, R. E., Huang, H., Anderson, B. E., Avery, M. A., Clarke, A. D., and Blake, D. R.: Impacts of aerosols and clouds on photolysis frequencies and photochemistry during TRACE-P: 2. Three-dimensional study using a regional chemical transport model, Journal of Geophysical Research: Atmospheres, 108, 8822, 10.1029/2002jd003100, 2003.

Turner, A. J., Frankenberg, C., Wennberg, P. O., and Jacob, D. J.: Ambiguity in the causes for decadal trends in atmospheric methane and hydroxyl, Proc Natl Acad Sci U S A, 114, 5367-5372, 10.1073/pnas.1616020114, 2017.

Turner, A. J., Fung, I., Naik, V., Horowitz, L. W., and Cohen, R. C.: Modulation of hydroxyl variability by ENSO in the absence of external forcing, Proceedings of the National Academy of Sciences, 115, 8931-8936, 10.1073/pnas.1807532115, 2018.

Turner, A. J., Frankenberg, C., and Kort, E. A.: Interpreting contemporary trends in atmospheric methane, Proceedings of the National Academy of Sciences, 116, 2805-2813, 10.1073/pnas.1814297116, 2019.

Wolter, K., and Timlin, M. S.: El Niño/Southern Oscillation behaviour since 1871 as diagnosed in an extended multivariate ENSO index (MEI.ext), International Journal of Climatology, 31, 1074-1087,

10.1002/joc.2336, 2011.

Yienger, J. J., and Levy II, H.: Empirical model of global soil-biogenic NOχ emissions, Journal of Geophysical Research: Atmospheres, 100, 11447-11464, 10.1029/95jd00370, 1995.

Zhang, T., Hoell, A., Perlwitz, J., Eischeid, J., Murray, D., Hoerling, M., and Hamill, T. M.: Towards Probabilistic Multivariate ENSO Monitoring, Geophysical Research Letters, 46, 10532-10540, 10.1029/2019gl083946, 2019.

Zhang, Z., Zimmermann, N. E., Calle, L., Hurtt, G., Chatterjee, A., and Poulter, B.: Enhanced response of global wetland methane emissions to the 2015–2016 El Niño-Southern Oscillation event, Environmental Research Letters, 13, 074009, 10.1088/1748-9326/aac939, 2018.

Zhao, Y., Saunois, M., Bousquet, P., Lin, X., Berchet, A., Hegglin, M. I., Canadell, J. G., Jackson, R. B., Hauglustaine, D. A., Szopa, S., Stavert, A. R., Abraham, N. L., Archibald, A. T., Bekki, S., Deushi, M., Jöckel, P., Josse, B., Kinnison, D., Kirner, O., Marécal, V., O'Connor, F. M., Plummer, D. A., Revell, L. E., Rozanov, E., Stenke, A., Strode, S., Tilmes, S., Dlugokencky, E. J., and Zheng, B.: Inter-model comparison of global hydroxyl radical (OH) distributions and their impact on atmospheric methane over the 2000–2016 period, Atmos. Chem. Phys., 19, 13701-13723, 10.5194/acp-19-13701-2019, 2019.

Zhao, Y., Saunois, M., Bousquet, P., Lin, X., Berchet, A., Hegglin, M. I., Canadell, J. G., Jackson, R. B., Dlugokencky, E. J., Langenfelds, R. L., Ramonet, M., Worthy, D., and Zheng, B.: Influences of hydroxyl radicals (OH) on top-down estimates of the global and regional methane budgets, Atmos. Chem. Phys. Discuss., 2020, 1-45, 10.5194/acp-2019-1208, 2020.

Zheng, B., Chevallier, F., Yin, Y., Ciais, P., Fortems-Cheiney, A., Deeter, M. N., Parker, R. J., Wang, Y., Worden, H. M., and Zhao, Y.: Global atmospheric carbon monoxide budget 2000–2017 inferred from multi-species atmospheric inversions, Earth Syst. Sci. Data, 11, 1411-1436, 10.5194/essd-11-1411-2019, 2019.

Ziemke, J. R., Oman, L. D., Strode, S. A., Douglass, A. R., Olsen, M. A., McPeters, R. D., Bhartia, P. K., Froidevaux, L., Labow, G. J., Witte, J. C., Thompson, A. M., Haffner, D. P., Kramarova, N. A., Frith, S. M., Huang, L. K., Jaross, G. R., Seftor, C. J., Deland, M. T., and Taylor, S. L.: Trends in global tropospheric ozone inferred from a composite record of TOMS/OMI/MLS/OMPS satellite measurements and the MERRA-2 GMI simulation, Atmos. Chem. Phys., 19, 3257-3269, 10.5194/acp-19-3257-2019, 2019.

Figures & Tables

Table 1. Two-box model inversion experiments.

Inversion experiments	OH variability
Inv_OH_std	Full temporal changes (scaled OH fields)
Inv_OH_cli	Climatology OH (average of 1980-2010)
Inv_OH_var	Year-to-year variation only (detrend OH fields)
Inv_OH_trend	Trend only (remove OH year-to-year variation)

675

Table 2. Multi-model mean ± standard deviation (SD) of annual total OH production (P) and loss (L) in Tmol yr^{-1} and percentage contribution of each production and loss processes to total OH production and loss estimated with multi-model mean OH fields[1].

Chemical reaction	**Mean ± SD**	**%**
Production	209 ± 12	/
$O(^1D)+H_2O$	96 ± 2	46%
$NO+HO_2$	63 ± 4	30%
O_3+HO_2	26 ± 3	13%
Other	24 ± 7	12%
Loss[1]	209 ± 12	/
$CO+OH$	82 ± 4	39%
CH_4+OH	32 ± 1	15%
CH_2O+OH	12 ± 1	6%
Isoprene+OH	13 ± 1	6%
Other	70 ± 5	33%

[1] The OH production and loss of the EMAC model are not included in the table since total OH production and loss are not given by the EMAC model.

680

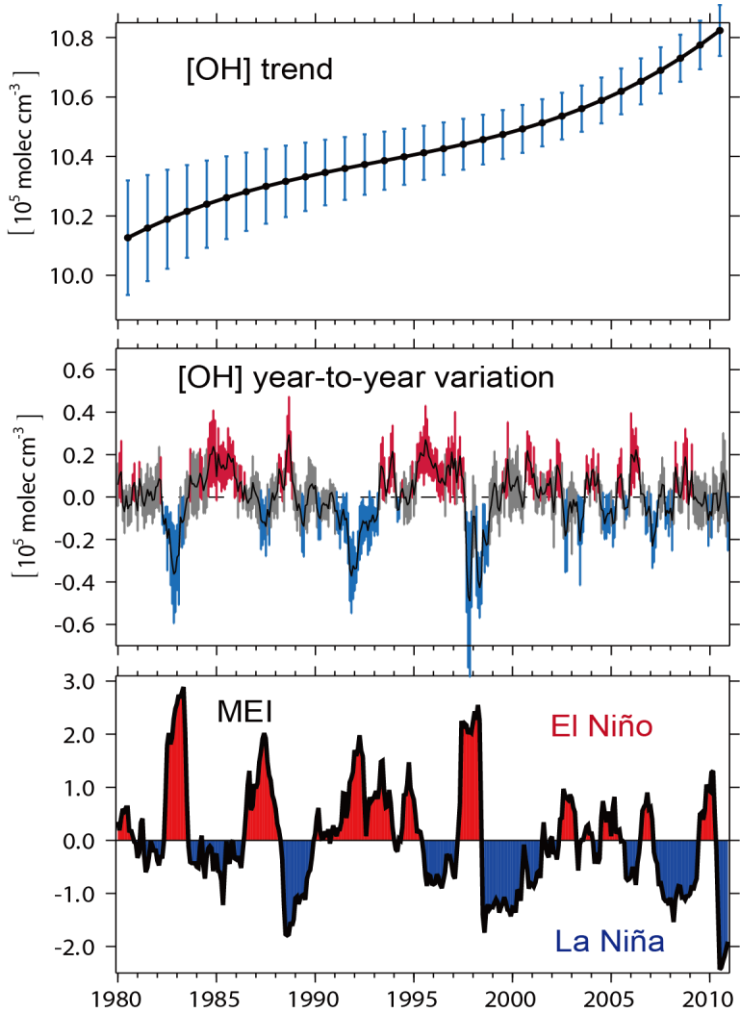

Figure 1. Top panel: Annual global tropospheric mean OH concentration ($[OH]_{GM\text{-}CH4}$, CH_4 reaction weighted) with year-to-year variations removed (represents the OH trend) simulated by CCMI models. The black line is the multi-model mean and associated error bars are standard deviations of different model results (also for the middle panel). Middle panel: Anomaly of detrended and deseasonalized monthly mean $[OH]_{GM\text{-}CH4}$ (represents the year-to-year variations of OH). Red bars indicate that the multi-model simulated $[OH]_{GM\text{-}CH4}$ are statistically significant ($P<0.05$) positive anomalies, blue bars indicate statistically significant negative anomalies, and grey bars indicate statistically non-significant anomalies. Bottom panel: Bi-monthly Multivariate ENSO Index (MEI).

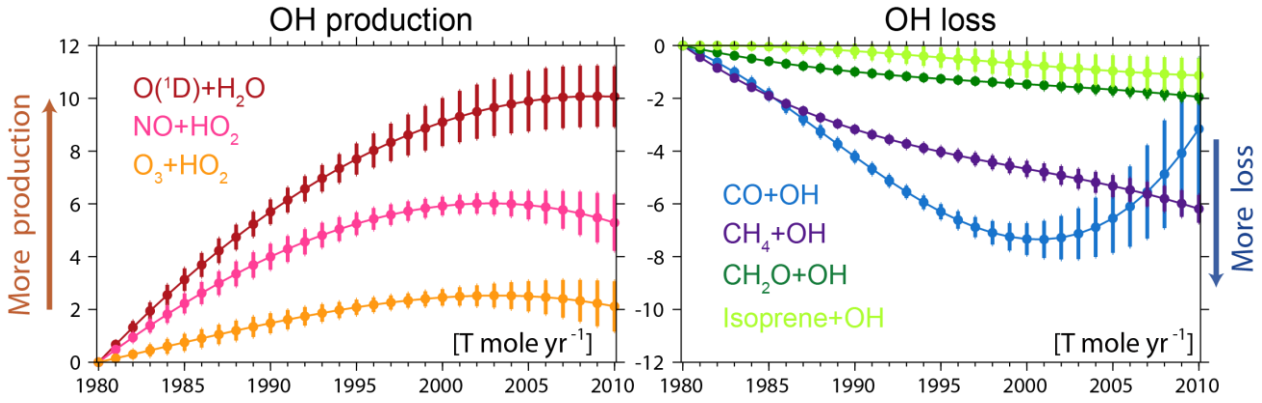

Figure 2. Annual total OH tendency (Tmole yr^{-1}) from chemical reactions with respect to the year 1980 with year-to-year variations removed. The positive and negative tendencies represent OH production (left) and loss processes (right), respectively.

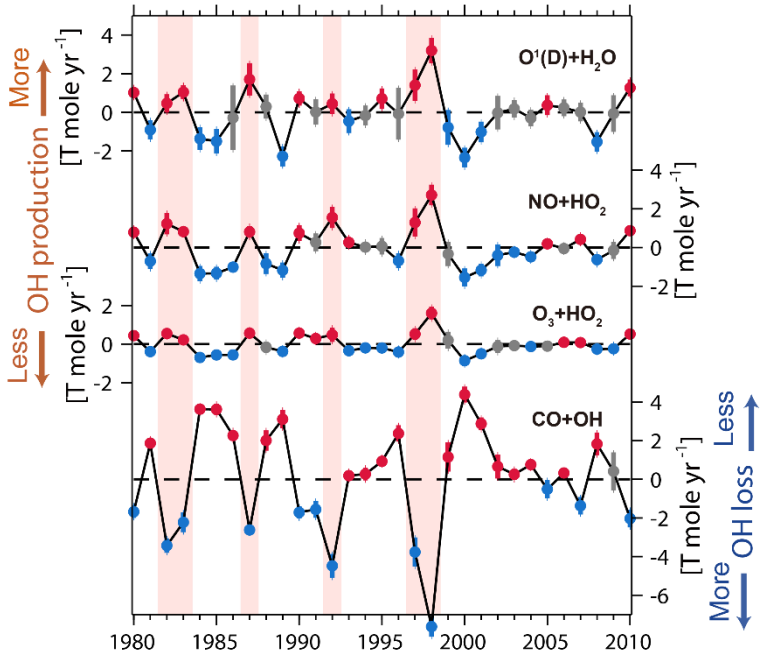

Figure 3. Anomaly of the detrended annual global total OH tendency from reactions $O(^1D)+H_2O$, $NO+HO_2$, O_3+HO_2, and CO+OH. The positive and negative tendencies represent OH production and loss processes, respectively. Black lines are multi-model means and the error bars are the standard deviations of all CCMI model results. The red, blue, and grey dots and error bars show statistically significant ($P<0.05$) positive anomalies, negative anomalies, and statistically non-significant anomalies, respectively. Shaded areas represent the El Nĩno years with more than 5 months of MEI>1.0.

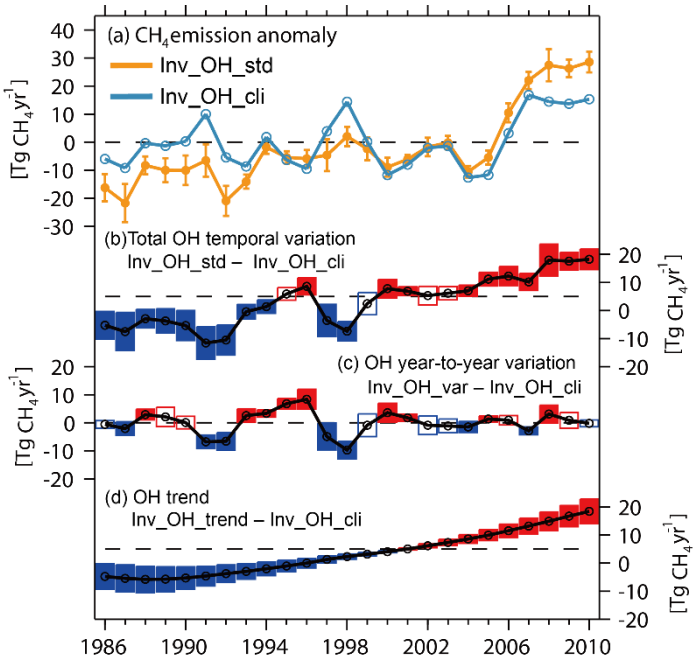

Figure 4. **(a)** Anomaly of global total CH_4 emissions using scaled CCMI OH fields (yellow line, Inv_OH_std), and climatological OH (blue, Inv_OH_cli) estimated by a two-box model inversion. The anomalies are calculated by comparing to the climatological mean CH_4 emissions of Inv_OH_cli over 1986-2010. **(b)** Influence of total OH temporal variations (OH year-to-year variation and trend, Inv_OH_std minus Inv_OH_cli), **(c)** OH year-to-year variations (Inv_OH_var minus Inv_OH_cli), and (**d)** OH trend (Inv_OH_trend minus Inv_OH_cli) on box-model estimated global total CH_4 emissions. The black lines are the mean of inversion results with different OH fields and the boxes are ±one standard deviation. The boxes with filled blue/red show OH lead to statistically significant ($P<0.05$) differences between the two inversions.

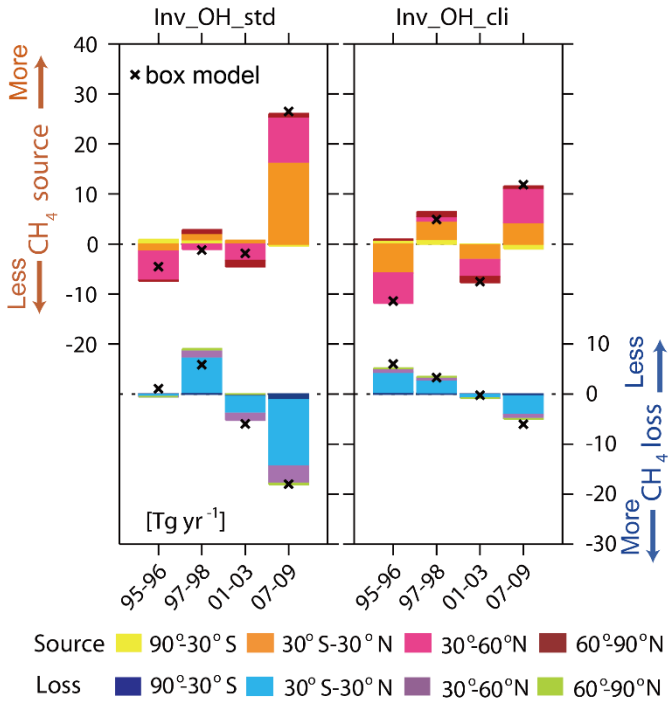

Figure 5. Anomaly of CH_4 emissions and losses estimated by variational 4D inversions (bars) and by two-box model inversions ("**x**") using a multi-model mean scaled OH (Inv_OH_std, left column) and climatological OH (middle column) during four time periods. The anomalies are calculated by comparing to the mean CH_4 emissions of Inv_OH_cli over the four time period (494Tg). The differences between Inv_OH_std and Inv_OH_cli (Inv_OH_std minus Inv_OH_cli) are presented in the right column. The total emissions and loss over southern extra-tropical regions (90 °S-30 °S), the Tropics (30 °S-30 °N), the northern temperate (30 °-60 °N), and the boreal (60 °-90 °N) regions are shown by different colors within each bar.